BRNO UNIVERSITY OF TECHNOLOGY

VYSOKÉ UČENÍ TECHNICKÉ V BRNĚ

FACULTY OF ELECTRICAL ENGINEERING AND COMMUNICATION
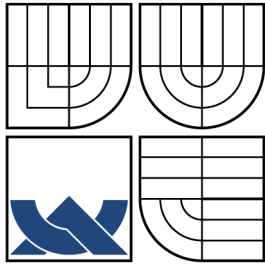## DEPARTMENT OF RADIO ELECTRONICS

FAKULTA ELEKTROTECHNIKY A KOMUNIKAČNÍCH TECHNOLOGIÍ
ÚSTAV RADIOELEKTRONIKY

EFFECT OF OPTICAL ELEMENTS ON TRANSMITTED LASER BEAM

MASTER'S THESIS
DIPLOMOVÁ PRÁCE

AUTHOR   Bc. et Bc. JURAJ POLIAK
AUTOR PRÁCE

BRNO UNIVERSITY OF TECHNOLOGY
VYSOKÉ UČENÍ TECHNICKÉ V BRNĚ

FACULTY OF ELECTRICAL ENGINEERING AND COMMUNICATION
DEPARTMENT OF RADIO ELECTRONICS

FAKULTA ELEKTROTECHNIKY A KOMUNIKAČNÍCH TECHNOLOGIÍ
ÚSTAV RADIOELEKTRONIKY

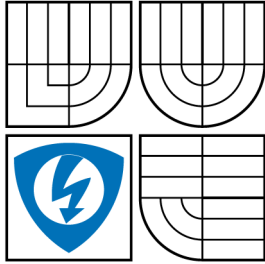# EFFECT OF OPTICAL ELEMENTS ON TRANSMITTED LASER BEAM
VLIV OPTICKÝCH PRVKU NA VYZAŘOVANÝ LASEROVÝ SVAZEK

MASTER'S THESIS
DIPLOMOVÁ PRÁCE

AUTHOR   Bc. et Bc. JURAJ POLIAK
AUTOR PRÁCE

SUPERVISOR   prof. Ing. OTAKAR WILFERT, CSc.
VEDOUCÍ PRÁCE

BRNO 2011

**VYSOKÉ UČENÍ
TECHNICKÉ V BRNĚ**

**Fakulta elektrotechniky
a komunikačních technologií**

Ústav radioelektroniky

Diplomová práce

magisterský navazující studijní obor
Elektronika a sdělovací technika

Student:	Bc. Juraj Poliak	*ID:*	78397
Ročník:	2	*Akademický rok:*	2010/2011

NÁZEV TÉMATU:

Vliv optických prvků na vyzařovaný laserový svazek

POKYNY PRO VYPRACOVÁNÍ:

Seznamte se s funkcí a skladbou optického spoje určeného k testování atmosférické optické komunikace. Pomocí vhodného programu modelujte rozložení optické intenzity v různých rovinách kolmých na osu vysílaného svazku a ověřte vliv difrakce na vysílací čočce.

Vytvořte program pro modelování difragovaného svazku v různých vzdálenostech měřicí roviny od vysílací apertury. Tuto vzdálenost volte s ohledem na hranici blízké a vzdálené zóny záření tak, aby výsledkem byly charakteristiky v obou zónách.

Předpokládejte, že kruhově symetrická vysílací čočka je ozařovaná elipticky symetrickým laserovým svazkem. Pomocí vytvořeného programu navrhněte optimální uspořádání vysílače s přiměřeným vlivem difrakce a přiměřenými výkonovými ztrátami. Svůj návrh experimentálně ověřte.

DOPORUČENÁ LITERATURA:

[1] SALEH, B. E. A. Základy fotoniky. Praha: Matfyzpress, 1995. ISBN 80-85863-00-6

[2] WILFERT, O., KOLKA, Z. Statistical model of free-space optical data link. In: Proc. of The International Symposium on Optical Science and Technology. Conference 5550. Denver: SPIE. 2004, p. 203-213.

Termín zadání:	7.2.2011	*Termín odevzdání:*	20.5.2011

Vedoucí práce: prof. Ing. Otakar Wilfert, CSc.

prof. Dr. Ing. Zbyněk Raida
Předseda oborové rady

ABSTRACT

Master's thesis deals with scalar diffraction theory and introduces an important solution of wave equation – elliptically symetrical Gaussian beam. In practical part, two approaches of diffraction model are used. The model will be experimentaly confirmed during experiment. In the final part, results of this experiment and simulation are criticaly discussed.

KEYWORDS

Diffraction, Elliptical Gaussian beam, Fresnel integral, Fourier transform, Bessel function.

ABSTRAKT

Diplomová práca pojednáva o skalárnej teórii difrakcie a zavádza dôležité riešenie vlnovej rovnice a to elipticky symetrický Gaussov zväzok. V praktickej časti bude popísané modelovanie difrakcie na kruhovom otvore dvoma rôznymi prístupmi. Model bude experimentálne overený experimentom. V záverečnej časti bude kriticky pojednané o výsledkoch experimentu a simulácie.

KLÍČOVÁ SLOVA

Difrakcia, Eliptický Gaussov zväzok, Fresnelov integrál, Fourierova transformácia, Besselova funkcia.

DECLARATION

I declare that I have elaborated my master's thesis on the theme of "Effect of optical elements on transmitted laser beam" independently, under the supervision of the master's thesis supervisor and with the use of technical literature and other sources of information which are all quoted in the thesis and detailed in the list of literature at the end of the thesis.

As the author of the master's thesis I furthermore declare that, concerning the creation of this master's thesis, I have not infringed any copyright. In particular, I have not unlawfully encroached on anyone's personal copyright and I am fully aware of the consequences in the case of breaking Regulation § 11 and the following of the Copyright Act No 121/2000 Vol., including the possible consequences of criminal law resulted from Regulation § 152 of Criminal Act No 140/1961 Vol.

Brno . . . .
(author's signature)

CONTENTS

LIST OF FIGURES

LIST OF TABLES

1 INTRODUCTION

Increasing demand for optical communication systems is observed in last decade. Whether it's for a practical reason (unlicensed band, directivity of transmission) or to obtain higher speed rate. During pointing and shaping the optical beam, there are many wave phenomena of light applied to describe its distribution along the path, mostly diffraction phenomena. As later will be described, this phenomena were observed already in 17th century a despite that, a man has still not been able fully describe all its effects.

Second part of the thesis deals with a description of laser beam using important solution of wave equation - gaussian beam. For simplicity, basic parameters will be introduced on circularly symetrical gaussian beam. In practice, to describe real situation more finely, elipticaly symetrical gaussian beams are used and will be discussed as well.

In the main part, two different approaches to simulate diffraction and its aspects will be introduced. First model uses Fourier transform of 2-dimensional signal and second one uses integral of Bessel functions. Results of both simulation will be compared.

Thesis concludes with a simulation of real beam and experimental verification of function of this program. The aim of this thesis will be to develop an application, which will is able to simulate diffraction effects and to test it on an experimental link.

2 DIFFRACTION

With description of electromagnetic radiation in free space deals optics. According to degree of abstraction, optics is further divided into:

- Geometric
- Wave
- Electromagnetic
- Quantum

Each area includes all previous areas. It would be then logical to use always knowledge of quantum optics to express all optics effects. That would lead to redundant effort, as usualy such a fine resolution would not be necessary. In some cases it is not even possible.

Electromagnetic radiation never distributes throughout infinite space. During its distribution it collides with obstacles and as will be discussed later, this interaction leads to interesting effects. The most common and most significant is diffraction.

Name for diffraction was created by the founder of diffraction F.M.Grimaldi in 1665. The word is consists of two parts: latin *dis-*, that means opposite, negation and *frangere*, thats main meaning is to bend. Grimaldi so characterised the light, that deviates from its straightforward distribution in another way than bending or refraction. In his book *"Physico-mathesis de lumine, coloribus, et iride"* (Physico-mathematical Studies of Light, Colors, and the Rainbow) wrote:

> "Lumen propagatur seu diffunditur non solum directe, refracte ac reflexe, sed etiam alio quodam quarto modo, diffracte."

> "Light propagates and spreads not only directly, through refraction, and reflection, but also by a fourth mode, diffraction."

This sentence up to this day defines the term of diffraction. For modern purposes is appropriate to add, that distribution via homogenous and isotropic enviroment is supposed and for the term of diffraction is used for light effect behind the obstacle limiting the optical beam.

2.1 Fresnel and Fraunhofer diffraction

In optics, two types of diffraction phenomena are distinguished. It's Fresnel and Fraunhofer diffraction. In this section, qualitative analysis of both will be discussed.

In case of screening of image, e.g. rectangle aperture (see fig.2.1) without any use of optics, shielding object μ with rectangle aperture is placed between light source P_0 and plane of observation π. Expectations of inexperienced would be, that the

projection of the aperture in the plane π would be more precise as the dimension of the light source P_0 decreases. However, when monochromatic light is used, in the plane π complex pattern (such as on fig.2.2) will be observed. The cause is bending of light on the obstacle and the fourth way of distribution of light occurs.
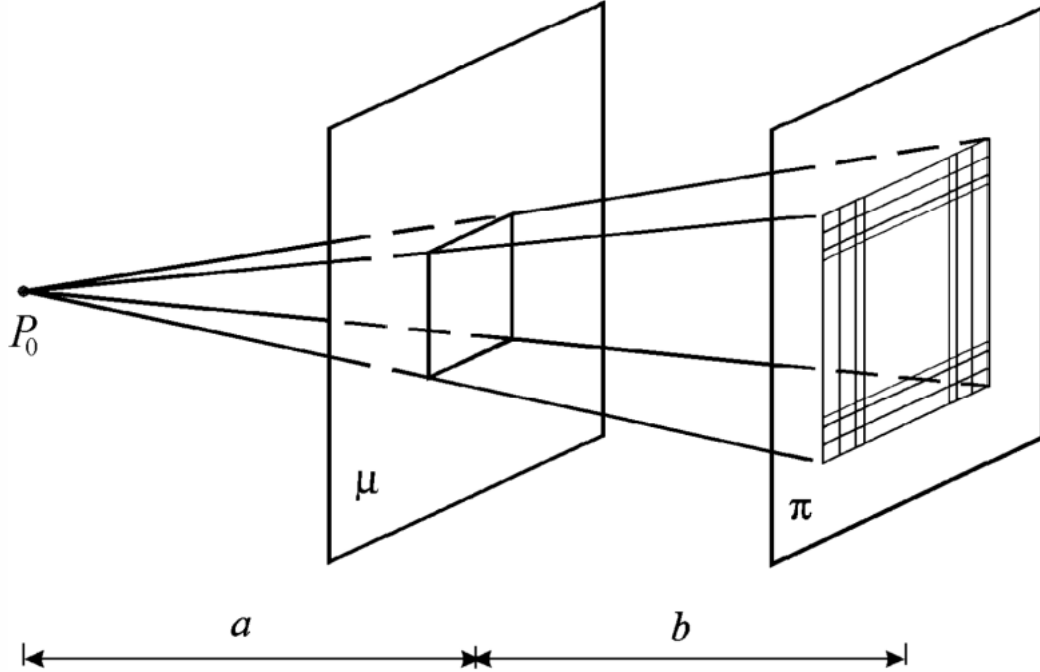
Fig. 2.1: Projection of aperture in the shielding object μ to plane of observation π. [1]

When small monochromatic coherent light source P_0 is used, Fresnel phenomena are apparent during shadow projection and in optical imaging systems are the main cause of blur and limit resolution of the whole system.

But problematics of Fraunhofer diffraction is more complex. In many cases it may be considered as special case of Fresnel diffraction. This phenomenon is so complex, that many scientists understand diffraction simply as Fraunhofer diffraction.

In the experiment on figure 2.1 one may increase the distance from source P_0 to the plane π as well as distance from the plane π to μ. Theoreticaly, one may increase these distances to infinity $(a, b \rightarrow \infty)$. Then, only planar wave approaching the plane of observation μ is considered and points in infinity will be considered as directions. Fraunhofer diffraction then represents distribution of light in direction to the point of observation, i.e. intensity of radiation distributing from the aperture to the observation plane in individual directions. In case of Fresnel diffraction, distribution of light as the function of location is considered. In practice, Fraunhofer pattern is achieved using lens.
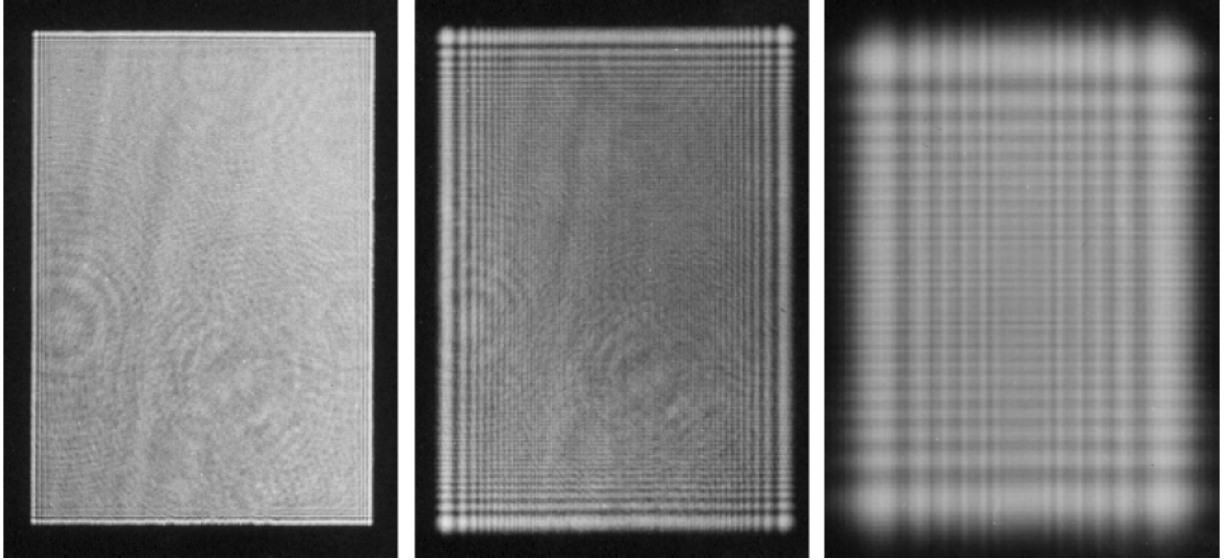
Fig. 2.2: Observation of Fresnel diffraction on rectangle aperture in opaque object obtained from the experiment on figure 2.1 for various combinations of values a a b. Dimension of aperture in the plane P_0 are 5.4 ×7.5 mm, $\lambda = 630$ nm.[1]

2.2 Huygens-Fresnel principle

Diffraction phenomena are usually derived from Huygens-Fresnel principle. Huygens in his work *"Traité de la lumiére"* (1690) was first who quantitatively expressed distribution of light in free space, reflection, refraction and birefringence (or double refraction). He used "Huygens constructions" (equivalent for Huygens principle). It includes two arguments:

I/ Every point of homogenous and isotropic enviroment, on which a wave (every point of wavefront) falls is considered to be a centre of secondary spherical wave.

II/ Wavefront at the time $t + \Delta t$ is a sum of secondary spherical waves at the previous time t.

The idea according to the second statement is obviously incorrect as it contradicts the observations of interference and diffraction phenomena.

Augustin Jean Fresnel was first who was able to explain all known diffraction phenomena. He achieved this with a change in the second Huygens' statement. Fresnel added, that secondary waveforms interfere with each other and specified amplitude and phase of secondary waveforms.

It is assumed, that enviroment in which the wave propagates is homogenous and isotropic dielectric medium. Optical wave is monochromatic, spherical, linearly poliarised and its optical intensity is so low, that it doesn't induce any nonlinear effects in that enviroment. Plane S defines position of planar wave at the time t.

Let in the points M of this plane be a known wave function $\psi_0(M)$ and it indicates a primary stimulus. From every point on the right side of the plane S secondary wave is coming out.

$$\psi(s, \vartheta) = -\frac{\mathrm{j}}{\lambda} K(\vartheta) \psi_0(M) \frac{e^{jks_M}}{s_M}, \qquad (2.1)$$

where the meaning of symbols is obvious according to the figure 2.3. Moreover, ϑ denotes the angle between normal to the plane S and direction s_{M}. $\frac{e^{jks_M}}{s_M}$ is devergent spherical wave coming from the point M.
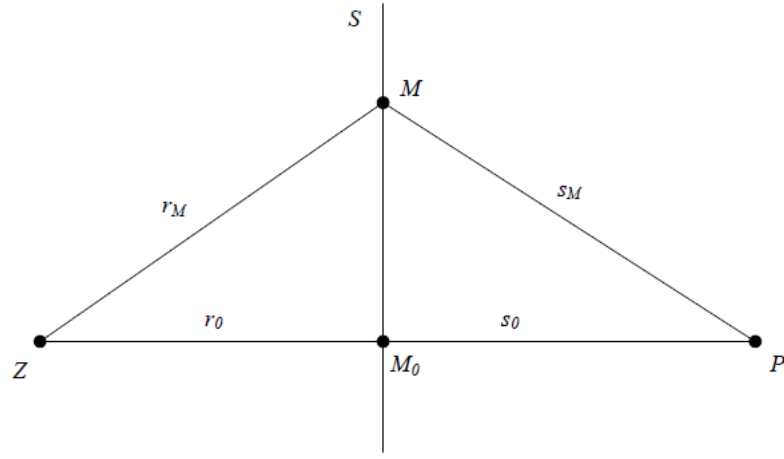
Fig. 2.3: Representation of Huygens-Fresnel principle. [2]

Term $-\frac{\mathrm{j}}{\lambda}$ indicates, that secondary waves' amplitude is inversely proportional to the wavelength and its phase outruns the phase of primary stimulus for quarter of a period. Fresnel introduced this factor to come to a correct solution in case no obstacle is present. $K(\vartheta)$ might be the most problematic factor and it was named slope factor. It indicates, that amplitude of secondary waves is depends on the direction of wave distribution. As the plane S Fresnel has chosen a wavefront. Then the angle ϑ would be the angle between normal to a wavefront at the point M and the direction determined by the connection of the point M and the point of observation P and the factor $K(\vartheta)$ assumed in the form of

$$K(\vartheta) = \begin{cases} \cos \vartheta & \text{pre } \vartheta \in \left\langle -\frac{\pi}{2}, \frac{\pi}{2} \right\rangle \\ 0 & \text{pre } \vartheta \in \left\langle \frac{\pi}{2}, \frac{3\pi}{2} \right\rangle \end{cases}. \qquad (2.2)$$

Nowadays the plane S is considered to be the plane of diffraction aperture.

Let S_0 be the part of the plane S, which is not shadowed with diffraction shield. According to Fresnel the wave function in the point P out of the plane S is given as sum of all secundary waves coming from the plane S_0, then:

$$\psi(P) = -\frac{jk}{2\pi} \iint\limits_{S_0} \psi_0(M) \frac{e^{jks_M}}{s_M} \cos \vartheta \ dS_0.$$ (2.3)

is a mathematical expression of Huygens-Fresnel principle.

2.3   Fresnel zones

To explain diffraction effect one has to fimiliarise himself with the term of Fresnel zone. It provides a better description of diffraction phenomena.

Let from the point source P_1 come a spherical wave out and S is one of its equiphase surface in the distance z_1. In the distance $z_1 + z$ from the source let be the point of observation P. Then, let $\sigma_0, \sigma_1, \sigma_2, \ldots$ be spherical waves with radius z, $z + \lambda/2$, $z + 2.\lambda/2$, $\ldots$ respectively around this point. These waves divide the equiphase surface S into zones. When $\psi_1, \psi_2, \psi_3, \ldots$ mark sums of these secondary waves coming to the point P from the first, second, third, $\ldots$ zone respectively, then it is obvious, that ψ_2 will have opposite phase, than ψ_1 and so on. Radius r_n of nth zone according to Pythagorean theorem (fig.3 [1]) would be:

$$\begin{aligned} (z_1 - \Delta)^2 + r_n{}^2 &= z_1{}^2 \\ (z + \Delta)^2 + r_n{}^2 &= \left(z + n\frac{\lambda}{2}\right)^2 \end{aligned}.$$ (2.4)

After the exclusion Δ:

$$r_n^2 = \frac{n\lambda z_1 z}{z_1 + z}\left[1 + \frac{1}{2}\left(\frac{n\lambda}{2}\right)\frac{z_1^2 + z_1 z - z^2}{z_1 z(z_1 + z)} - \frac{1}{2}\left(\frac{n\lambda}{2}\right)^2 \frac{1}{z_1(z_1 + z)} - \frac{1}{8}\left(\frac{n\lambda}{2}\right)^3 \frac{1}{z_1 z(z_1 + z)}\right].$$ (2.5)

Quantitative analysis shows, that terms of second, third and fourth order may be excluded. Then radius of nth zone is

$$r_n = \sqrt{\frac{n\lambda z_1 z}{z_1 + z}}.$$ (2.6)

Them Fresnel zones on the wavefront S are approximately planar:

$$\pi\left(r_n^2 - r_{n-1}^2\right) = \pi \frac{\lambda z_1 z}{z_1 + z}.$$ (2.7)

That also concludes, that sums ψ_i of secondary waves coming from these zones to the point P have the same absolute value. Then, when through the opaque shield

exactly first two zones penetrate, wave function in the point P will be zero, because sums ψ_1 a ψ_2 have the same absolute value, but opposite phase. That means, that optical intensity will be zero as well. The same situation repeats when even number of Fresnel zones is transmitted through the aperture.

Construction of Fresnel zones leads to a conclusion, that when aperture in the shield is increased from zero radius, intensity at the point of observation P increases until exactly first Fresnel zone is transmitted. When the radius is further increased, optical intensity at the point P decreases to zero when the second Fresnel zone is transmitted. When the radius is increased even more, the whole process repeats. Maximum modulus of wave function aplitude occurs when odd number of Fresnel zones is transmitted.

This maximum intensity is derived in [1], section 5.8.1.. Here, the expression as Fresnel formulated it will be mentioned. Despite of inaccurate reasoning, this expression appeared to be correct. When through the circular aperture an odd number of Fresnel zone is transmitted, optical intensity at the point of observation P is quadruple compared with optical intensity that would be at this place in case of no shield present, i.e. that wave function would be double. This implies, that if only half of the first Fresnel zone is transmitted, there would be the same optical intensity at the point P as for not obscured wave. This result Fresnel assumed and supported it with an assumption, which was not correct and Fresnel knew it. He calculated contribution ψ_i of individual zones:

$$\psi(P) = \frac{1}{2}\psi_1 + \left(\frac{1}{2}\psi_1 + \psi_2 + \frac{1}{2}\psi_3\right) + \cdots + \psi_\vartheta = \frac{1}{2}\psi_1, \qquad (2.8)$$

and a half of a contribution of the last zone

$$\psi_\vartheta = \frac{1}{2}\psi_n, \text{ resp. } \psi_\vartheta = \frac{1}{2}\psi_{n-1} + \psi_n$$

left out. He justified this with zero value of a slope factor $K(\vartheta) = \cos\vartheta$ for $\vartheta = \pi/2$.

Simply contribution of wave function from each even zone compensated with contributions from halfs of adjacent odd zones. Result, even when not derived mathematically correctly, represents the reality. This illustrates meaning of surrounding of the point M_0 (point of stationary phase) for the wave function at the point of observation P.

When the planar incident wave is considered, surface S is planar and from the Pythagorean theorem can be for outer radius r_n of nth Fresnel zone derived following expression:

$$r_n = \sqrt{n\lambda z}\sqrt{1 + \frac{n\lambda}{4z}}. \qquad (2.9)$$

One may with high accuracy presume, that

$$r_n = \sqrt{n\lambda z}. \tag{2.10}$$

2.4 Derivation of diffraction integrals

In following section diffraction integrals for Fraunhofer and Fresnel diffraction will be derived.

In the integral 2.3 stands as integral area S_0 usualy nonshielding part of wavefront or diffraction shield. In this derivation, as an integral area, the part of a plane that corresponds with transparent parts of the shade will be taken and this plane will be considered as the axis plane $z = 0$.
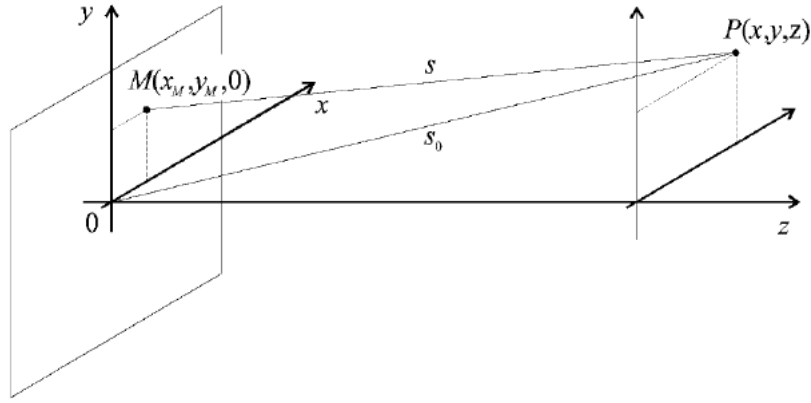
Fig. 2.4: Representation of Fresnel diffraction integral derivation. [1]

The slope factor is assumed to be $K(\vartheta) = 1$. Expression 2.3 is now as follows:

$$\psi(P) = -\frac{\mathrm{j}k}{2\pi} \iint\limits_{S_0} \psi_0(x_M, y_M) \frac{e^{jks_M}}{s_M} \, \mathrm{d}x_M \, \mathrm{d}y_M. \tag{2.11}$$

When the spherical wave in the equation 2.11 is substituted with its Fresnel approximation [1]:

$$\frac{e^{jks_M}}{s_M} \approx \frac{e^{jkz}}{z} e^{\frac{\mathrm{j}k}{2z}[(x-x_M)^2+(y-y_M)^2]}, \tag{2.12}$$

where $\psi_0(x_M, y_M) = 0$ at the points of opaque part of the shade.

Diffraction integral for Fresnel diffraction phenomena is now at following form:

$$\psi(x, y, z) = -\frac{\mathrm{j}k}{2\pi} \frac{e^{jkz}}{z} \iint\limits_{S_0} \psi_0(x_M, y_M) e^{\frac{\mathrm{j}k}{2z}[(x-x_M)^2+(y-y_M)^2]} \, \mathrm{d}x_M \, \mathrm{d}y_M. \tag{2.13}$$

From this expression on may proceed also when analytical calculation of wave function characterising some typical Fresnel diffraction effects. These calculations are not very straightforward as they use special functions - Fresnel integrals, Bessel and Lommel functions. Not even numerical calculations would be simple. There is a simple way to modify this expression to Fourier integral: One has to expand square power in the phasor argument and that leads to

$$\psi(x,y,z) = -\frac{\mathrm{j}k}{2\pi}\frac{e^{jkz}}{z}e^{\frac{\mathrm{j}k}{2z}(x^2+y^2)}\iint\limits_{S_0}\psi_0(x_M,y_M)e^{\frac{\mathrm{j}k}{2z}(x_M^2+y_M^2)}e^{-\frac{\mathrm{j}k}{z}(xx_M+yy_M)}\ \mathrm{d}x_M\ \mathrm{d}y_M.$$

(2.14)

Wave function characterising Fresnel diffraction is then expressed using Fourier transform of products of wave function ψ_0 on the plane of diffraction aperture and the phasor $e^{\frac{\mathrm{j}k}{2z}(x_M^2+y_M^2)}$.

Derivation of diffraction integral for Fraunhofer diffraction using Huygens-Fresnel principle is not as elegant as widespread. It proceeds, same as derivation of Fresnel diffraction integral, from the approximation of spherical wave. This time in a different way. The distance s_0 between the points M and P can be expanded in power series [1].

When the function $\psi_0(x_M,y_M)$ has nonzero values only close to origin O, as it can be in case of apertures in an opaque shade, specificaly if

$$\left.\frac{k(x_M^2+y_M^2)}{2s_0}\right|_{\max} \ll 2\pi,\quad \mathrm{tj.}\quad \left.\sqrt{x_M^2+y_M^2}\right|_{\max} \ll \sqrt{2\lambda s_0},$$

(2.15)

one may vanish terms containing integral variable of second and higher order in exponent of spherical wave expression and then the spherical wave can be expressed as follows

$$\frac{e^{jks_M}}{s_M} \approx \frac{e^{jks_0}}{s_0}e^{-\mathrm{j}k\left(\frac{x}{s_0}x_M+\frac{y}{s_0}y_M\right)}.$$

(2.16)

Using this expression has integral 2.11 shape of Fourier transform:

$$\psi(P) = -\frac{\mathrm{j}k}{2\pi}\frac{e^{jks_0}}{s_0}\iint\limits_{S_0}\psi_0(x_M,y_M)e^{-\mathrm{j}k\left(\frac{x}{s_0}x_M+\frac{y}{s_0}y_M\right)}\ \mathrm{d}x_M\ \mathrm{d}y_M.$$

(2.17)

Considering

$$\frac{x}{s_0} = n_x,\quad \frac{y}{s_0} = n_y,$$

(2.18)

19

where $\left(n_x, n_y, \sqrt{1 - n_x^2 - n_y^2}\right)$ are direction cosines of the direction $\vec{OP}$ and when the condition 2.15 is satisfied, the expression in front of the integral 2.17 is constant and wave function ψ is a function of direction cosines n_x, n_y and is in a form

$$\psi(P) = C \iint\limits_{S_0} \psi_0(x_M, y_M) e^{-\mathrm{j}k(n_x x_M + n_y y_M)} \, \mathrm{d}x_M \, \mathrm{d}y_M. \tag{2.19}$$

After closer look at the condition 2.15 is obvious, that Fraunhofer diffraction occurs only when linear dimension of aperture are relatively small with respect to the diameter of the first Fresnel zone. Within this context, Fresnel number N_f is defined as

$$N_f = \frac{a^2}{\lambda z}, \tag{2.20}$$

where a is radius of the circle, where shade has nonzero values of the transmission function a z is distance of this aperture from the plane of observation. It is used to determine which type of diffraction is observed. When Fresnel number is $N_f \geq 1$, it is mostly Fresnel diffraction. In case of $N_f < 1$ or rather $N_f \ll 1$ Fraunhofer diffraction is observed, except the case when the plane of observation is simultaneously plane of geometrical image of the source.

When in the equation 2.19 k is substituted for $k = \frac{2\pi}{\lambda}$ and introducing spatial frequencies

$$u = \frac{n_x}{\lambda}, \quad v = \frac{n_y}{\lambda}, \tag{2.21}$$

one leads to an equation

$$\psi(P) = C \iint\limits_{S_0} \psi_0(x_M, y_M) e^{-\mathrm{j}2\pi(u x_M + v y_M)} \, \mathrm{d}x_M \, \mathrm{d}y_M, \tag{2.22}$$

that expresses the relation between Fraunhofer diffraction and 2-dimensional Fourier transform.

3   GAUSSIAN BEAM

In this chapter, fundamental characteristics of laser beam, more specifically Gaussian beam, will be introduced. Gaussian beam is the simplest and most widely used approximation of real laser beam. Its origin is in the solution of wave equation for paraxial waves. First, circularly symmetrical beam is introduced followed by elliptically symetrical Gaussian beam.

3.1   Parameters of Gaussian beam

Optical power of Gaussian beam is focused into narrow cone and optical intensity I in a plane upright to the direction of propagation is given as a circularly symmetrical Gaussian function with a maximum I_0 on the axis of beam. This axis is determined by axis $0z$ of system of coordinates $0xyz$.

Beam halfwidth is from the designers' point of view one of the most interesting parameters. Laser beam can not be described as a ray, but as a beam, whose width changes during propagation. First, edge of the beam needs to be determined. It's given as a point where optical intensity decreases to the level $\frac{I_0}{e^2}$. Then beam halfwidth w is a distance from the beam axis to edge of the beam. Gaussian beam has the smallest value of beam halfwidth at the beam waist w_0. Beam waist is located on a plane $x0y$ and determines the origin of the coordinate system. Mathematically, in case 2-dimensional wave function is considered, following expression applies

$$\psi(x, z) = \psi_0 \sqrt{\frac{2}{\pi}} \frac{w_0 e^{-\mathrm{j}[\theta_0 - \theta(z)]}}{w(z)} e^{-\mathrm{j}\frac{kx^2}{2R(z)} - \frac{x^2}{w^2(z)}}, \tag{3.1}$$

where k is wave number mentioned above, $w(z)$ halfwidth of beam in the distance z and parameters $R(z)$ and $\phi(z)$ are curvature radius and beam divergency described below, respectively. Real part of exponential function determines evolution of intensity along transverse direction and imaginary part relates to a phase of the beam. Then, the relation of amplitude of wave function and optical intensity is

$$\psi(x, z) \propto e^{-\frac{x^2}{w^2(z)}}, \tag{3.2}$$

$$I(x, z) = |\psi(x, z)|^2. \tag{3.3}$$

Beam half-width $w(z)$ in the distance z is

$$w(z) = w_0 \sqrt{1 + \left(\frac{z\lambda}{\pi w_0^2}\right)^2} = \left| \frac{\pi w_0^2}{\lambda} = z_0 \right| = w_0 \sqrt{1 + \left(\frac{z}{z_0}\right)^2}, \tag{3.4}$$

where z_0 expresses the boundary between near and far field, i.e. Rayleigh distance. In this distance also $w(z_0) = w\sqrt{2}$ applies. This distance is the boundary between Fresnel and Fraunhofer region. This paper deals with diffraction effects in the distance less than z_0.
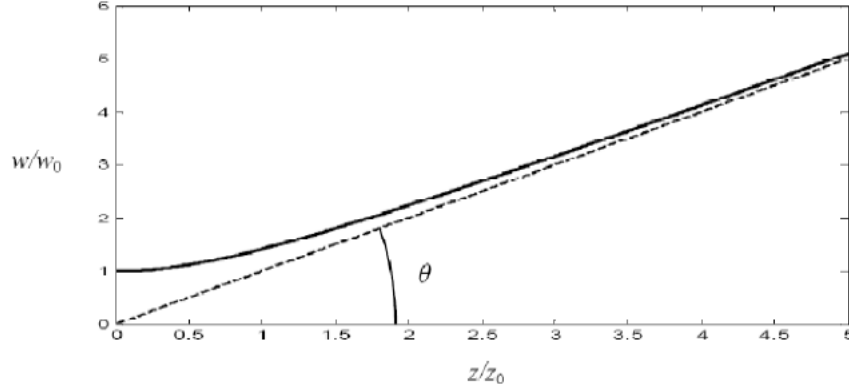
Fig. 3.1: Dependency of relative beam half-width on dimensionless coordinate z/z_0. [2]

The angle θ, which is the angle between the asymptote and axis x and is called beam divergency. For the beam divergency, following expression applies

$$\theta = \lim_{z \to \infty} \frac{w(z)}{z} = \frac{2}{kw_0} = \frac{\lambda}{\pi w_0}. \tag{3.5}$$

Wavefronts of Gaussian beam are close to the origin almost planar with radius of curvature $R \to \infty$. These wavefronts are bending as the wavefront propagates to both sides from the origin as denotes fig. 3.2. Gaussian beam wavefront curvature is maximum in Rayleigh distance. Radius of curvature in this distance is $R(z_0) = 2z_0$. It's evolution along the direction of propagation is given as follows

$$R(z) = z + \left[1 + \left(\frac{z_0}{z} \right)^2 \right]^2. \tag{3.6}$$

Gaussian beam is fully determined by beamwidth $w(z)$ and radius of curvature $R(z)$. These parameters may be unified in one complex parameter - complex radius of curvature given as

$$\frac{1}{\dot{q}(z)} = \frac{1}{R(z)} - j\frac{2}{kw^2(z)} = \frac{1}{R(z)} - j\frac{\lambda}{\pi w^2(z)} \tag{3.7}$$

3.2 Elliptically symmetrical Gaussian beam

In the previous chapter circularly symmetrical distribution of beam wave function ψ amplitude was assumed. That means, that in any plane upright to the direction
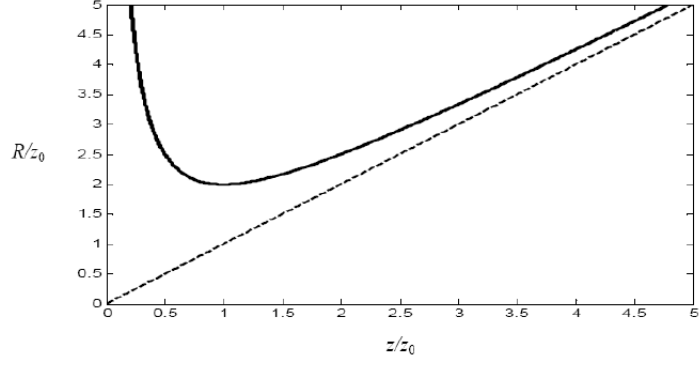
Fig. 3.2: Dependency of relative Gaussian beam radius of curvature on dimensionless coordinate z/z_0. [2]

of propagation, one is able to determine beam parameters as introduced above and independetnly on selection of this plane, these parameters are constant. Although this approximation simplifies calculations, it does not correspond with reality.

Better approximation of real laser beam is elliptically symmetrical Gaussian beam. There will be not only one parameter of beamwidth, but two: beam half-width w_x, and w_y at the x-axis and y-axis respectively. Amplitude of wave function will also change from 3.2 to

$$\psi(x, y, z) \propto e^{-\frac{x^2}{w_x^2(z)} - \frac{y^2}{w_y^2(z)}}. \tag{3.8}$$

Interesting is, that orientation of semi-major axis (in the cut of the plane upright to direction of propagation) will change after reaching the point, where both half-widths are equal and cut through this plane is circular.
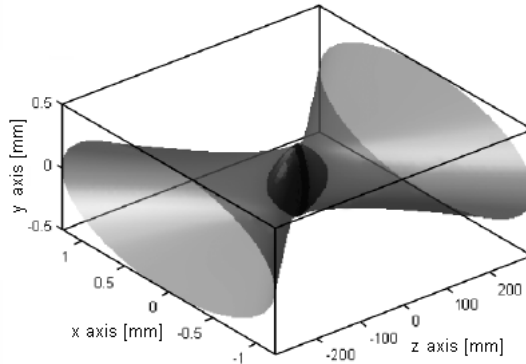
Fig. 3.3: Spatial dependency of elliptically symmetrical Gaussian beam half-width (modified from [3])

.

4 MODELLING OF DIFFRACTION

4.1 Limits and conditions of validity

For modelling of diffraction phenomena is from authors' point of view the most suitable to use MATLAB programme. It provides suitable enviroment, prearranged commands to image processing, integral calculation, Fourier transform as well as Bessel functions.

Before starting to write a programme itself, one has to be aware of all limitations, approximations and conditions when to use a desired expression. Diffraction is a phenomenon so complex, that to obtain accurate results, many aspect have to be analysed. On one hand, the phenomena should be described as generally as possible. But on the other hand, redundant complexity may lead to loss of contact between theory and reality. Therefore, limitations of expression describing diffraction have to be analysed.

Let assume diffraction of monochromatic planar wave with elliptically symmetrical Gaussian distribution of optical intensity around the origin common with the center of diffraction aperture. First, one has to be aware of coherence degree of laser beam. Therefore, spatial and time coherence is discussed at first.

4.1.1 Coherence

Common lasers used in practice have spectral width of order 10^{-10} m and they emmit radiation with wavelength of order 10^{-6} m. Degree of coherence therefore will be as follows

$$\frac{\Delta\lambda}{\lambda} = \frac{10^{-10}}{10^{-6}} = 10^{-4}, \tag{4.1}$$

that is a degree of coherence, that one may conclude, that laser beam is time-coherent. Then, average wavelentgh λ may be used in previous expressions.

Size of the elliptical area, from which laser radiation is emitted to space is critical to determine degree of spatial coherence. Its size is usualy of order 10^{-6} m. In practice, this radiation is observed in approximately 10^0 m. Considering ratio of these dimensions, one may consider the laser beam is radiated from a single point, i.e. laser is a point source.

4.1.2 Wavefront shape

To obtain planar wavefront at the transmitting aperture, the laser source has to be placed in infinity. Practically is this obtained using plan-convex lens and placing

the source to focus of this lens. This will ensure constant phase distribution at all points of diffraction apertures, which is an assumuption to use planar wave in the calculations. This assumption must be fulfiled.

Although, in practice the laser beam is slightly divergent in order of ones of miliradians. This allows easier pointing and to avoid other wave behaviour effects related to Heisenberg indeterminancy principle.

4.2 Choice of models

Model needs to be selected with respect to computational power and complexity of problem.

Exact Reyleigh-Sommerfeld integral as follows

$$\psi(x,y,z) = -\frac{\mathrm{j}kz}{2\pi} \iint f(x_M, y_M) \frac{\exp(\mathrm{j}k\sqrt{(x-x_M)^2 + (y-y_M)^2 + z^2})}{(x-x_M)^2 + (y-y_M)^2 + z^2} \times$$
$$\times \left[1 + \frac{\mathrm{j}}{k\sqrt{(x-x_M)^2 + (y-y_M)^2 + z^2}} \right] \mathrm{d}x_M \mathrm{d}y_M \tag{4.2}$$

is redundant. Its use would require for every point on observation plane double integral of complex function to be calculated.

4.2.1 Model based on FFT

For purposes of diploma thesis is most appropriate to work with Fresnel approximation (see section 2.4). Based on equation 2.14 one obtains

$$\psi\psi*(x,y,z) = C \left| \iint \mathrm{circ}\left(\frac{x_M^2 + y_M^2}{\rho_0^2}\right) \exp\left[\frac{2\pi\mathrm{j}}{2\lambda z}\left(x_M^2 + y_M^2\right)\right] \times \right.$$
$$\left. \times \exp\left[-\frac{2\pi\mathrm{j}}{\lambda z}\left(xx_M + yy_M\right)\right] \mathrm{d}x_M \mathrm{d}y_M \right|^2, \tag{4.3}$$

where C is a constant and ρ_0 radius of diffraction aperture.

Then from the equation 2.10 to intraduce distance z

$$z(n) = \frac{\rho_0^2}{n\lambda}, \tag{4.4}$$

where n is number of transmitted Fresnel zones.

Final equation would be

$$\psi\psi * (x, y, z) = C \left| \iint \text{circ}\left(\frac{x_M^2 + y_M^2}{\rho_0^2}\right) \exp\left[\frac{n\pi j}{\rho_0^2}\left(x_M^2 + y_M^2\right)\right] \right.$$
$$\left. \exp\left[-\frac{2\pi n j}{\rho_0^2}\left(xx_M + yy_M\right)\right] \mathrm{d}x_M \mathrm{d}y_M \right|^2 . \tag{4.5}$$

Function *circ* in the expression 4.5 represents circular diffraction aperture and it's defined as follows

$$\text{circ}(x) = \begin{cases} 1 & \text{for } x \le 1 \\ 0 & \text{for } x < 0 \end{cases} . \tag{4.6}$$

The term $\exp\left[-\frac{2\pi n j}{\rho_0^2}\left(xx_M + yy_M\right)\right]$ in the equation 4.5 is phase term derived from Fresnel approximation of diffraction integral. Last term in this equation is the term similar to term represented in Fourier transform. Then, one may write

$$\psi\psi * (x, y, z(n)) \propto \left| \mathcal{F}\left\{ \text{circ}\left(\frac{x_M^2 + y_M^2}{\rho_0^2}\right) \exp\left[j\frac{n\pi}{\rho_0^2}\left(x_M^2 + y_M^2\right)\right] \right\} \right|^2 . \tag{4.7}$$

Formulation based on number of Fresnel zones is practical during process of studying diffraction phenomena as it is illustrative approach. But this approach is not usable in practice, when distance z from the plane of shade, i.e. distance of receiver from the transmitter needs to be determined.

When equation 4.4 and $k = \frac{2\pi}{\lambda}$ apply, then

$$\frac{n\pi}{\lambda} = \frac{k}{2z}. \tag{4.8}$$

And finally

$$\psi\psi * (x, y, z(n)) \propto \left| \mathcal{F}\left\{ \text{circ}\left(\frac{x_M^2 + y_M^2}{\rho_0^2}\right) \exp\left[j\frac{k}{2z}\left(x_M^2 + y_M^2\right)\right] \right\} \right|^2 . \tag{4.9}$$

For purposes of implementation of Fourier transform in computer science, algorith of Fast Fourier Transform (FFT, see more in [4], section 8.4) was developed. It's used when real-time image processing is needed, also in fast spetroscopes.

AS it was already mentioned above, programme was developed in MATLAB enviroment as a GUI. In the window one only has to fill all the parameters and push the appropriate button. Functionality of the script is described below.

Program itself consists of several parts. In the first one, input parameters of physical meaning, e.g. wavelength *lambda*, radius of diffraction aperture r, distance

z_real, beamwidth in x-axis and y-axis plane *wx* and *wy*, are defined. There are also signal discretisation parameters such as size of plane object plane *range* and number of discretisation points N, defined.

In the following part, parameters needed for calculations are evaluated. These parameters are: wave number k, step of discretisation *delta*, distance in units of points z and *scale*, that is needed to determine range of display. Step of discretisation is needed to convert from real units, e.g. meter to display units (point or pixel) and vice versa. The relation between these is as follows

$$x_m = x_p \Delta, \tag{4.10}$$

where x_m is quantity expressed in real units, x_p is quantity expressed in display units and Δ is step defined as

$$\Delta = \frac{range}{N}, \tag{4.11}$$

Furthermore, diffraction aperture is defined

```
1 DP = zeros(N,N); % object plane of diffraction object
2 [x y] = meshgrid(-N/2:N/2-1,-N/2:N/2-1); % definition of
      object plane
3 s = sqrt((x+1) .* (x+1) + y .* y);
4 DP(s <= r/delta) = 1; % execution of circ(x) function
5 %% Gaussian distribution
6 wx = wx/delta;
7 wy = wy/delta;
8 G2 = zeros(N,N);
9 %% Fast Fourier Transform
10 FF = zeros((N+1)/2);
11 x = 0; y = 0;
12 for x = 1:size(DP,1)
13         for y = 1:size(DP,2)
14                 G2(y,x) = exp(-(((x-(N+1)/2)^2/(2*wx^2))+((y
                    -(N+1)/2)^2/(2*wy^2))));
15                 FF(y,x) = G2(y,x) * DP(y,x)*(exp(i*k/(2*z)
                    *((x-N/2)^2+(y-N/2)^2)));
16         end
17 end
18 F = fftshift((abs(fft2(FF))));
19 F = F.^2;
```

Gaussian distribution of intensity is defined by beamwidth already in the beginning of the program. Matrix of zero elements has to be created, that will be filled with calculated values of Gaussian distribution. Also, real quantities have to be converted to point units again.

Then, diffraction pattern is calculated using FFT algorithm.

Function $fft2$ evaluates spectrum so that areas corresponding to zero frequency are located in the corners. It is desirable to display this area in the center of the image. Therefore $fftshift$ function is used to rearrange individual quadrants.

Finaly, the script ends with functions to display graphs. Graphs display in general elliptically symmetrical incident laser beam on the upper left corner and circularly symmetrical aperture on the right. Distribution of diffraction pattern in the determined distance z is in the center. On the bottom, there are two one-dimensional distributions of this pattern accross the centre in horizontal and vertical axis, respectively.

On figure 4.1 are displayed results of monochromatic planar wave diffraction simmulation with parameters $\lambda = 830$ nm, $w_x = 20$ mm a $w_y = 40$ mm, $r = 30$ mm in the distance $z = 361,44$ m (exactly 3 Fresnel zones). It is obvious how choice of the beamwidth compared with aperture radius affects diffraction pattern.

4.2.2 Model based on integration of Bessel function

Bessel function $Z_\nu(z)$ of ν-th order are solution of differential equation

$$z^2 Z_\nu''(z) + z Z_\nu'(z) + \left(z^2 - \nu^2\right) Z_\nu(z) = 0. \tag{4.12}$$

Bessel functions are very important, because many situations, that have rotational or spherical symmetry, lead to Bessel equation and Bessel functions. Optical systems often show rotational symmetry, therefore one may use Bessel functions to solve them.

It can be shown ([5] Appendix B), that particular integral of this equation is in the form

$$Z(x) = J_\nu(x) = \frac{(-1)^k}{k!\Gamma(\nu + k + 1)} \left(\frac{x}{2}\right)^{\nu + 2k}, \tag{4.13}$$

and is called Bessel function of the first kind of the ν-th order. Besides that, there are also Bessel function of the second and third kind as well as of half-integer orders when $\nu = n \pm 12$. For better description, see [5]. Course of the Bessel function of the first kind is on the figure 4.2.

There are limits of using Bessel function of the first kind resulting from what was already mentioned above - restriction to rotationaly symmetrical situations. That
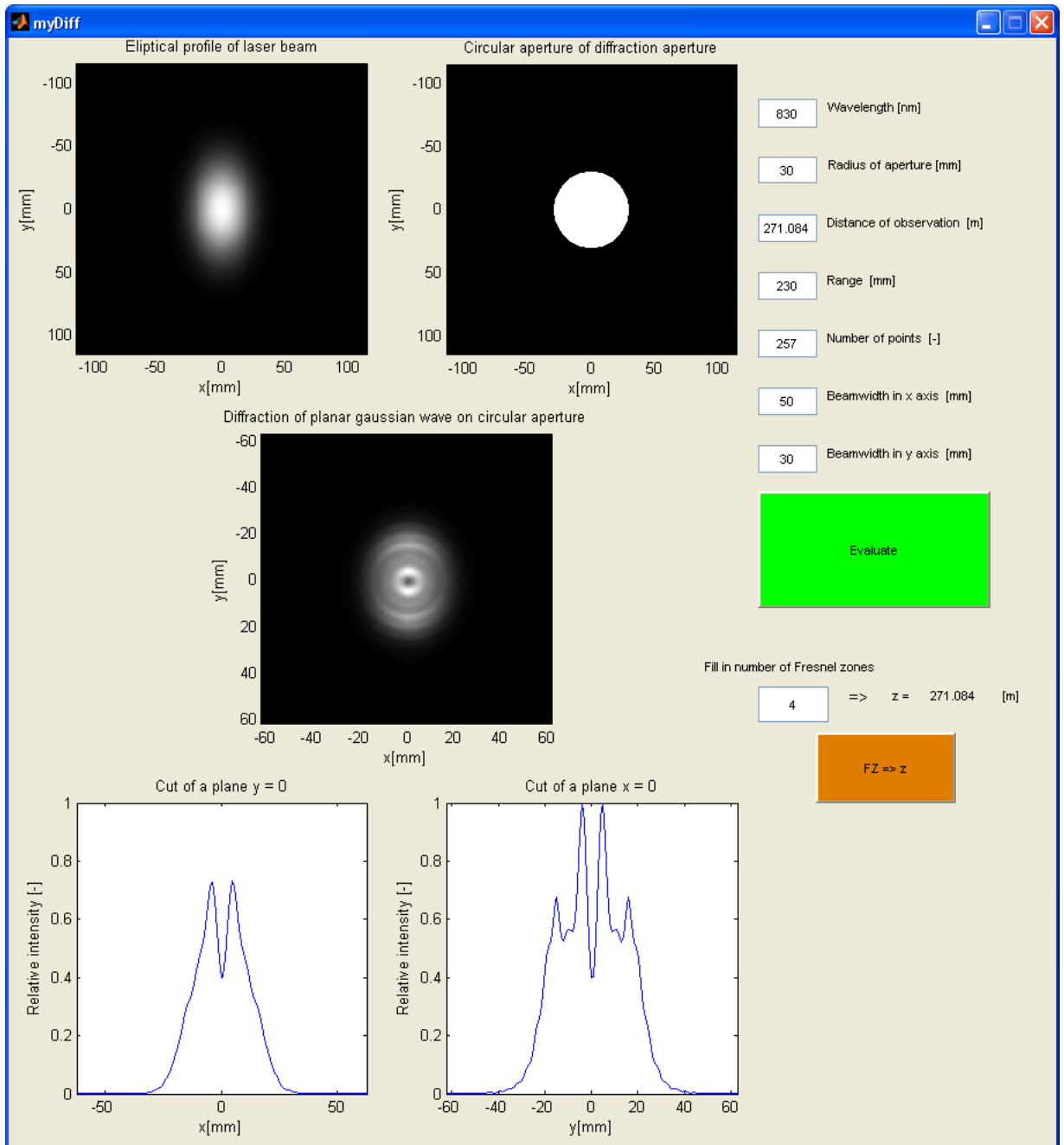
Fig. 4.1: Results of simulation using MATLAB script with parameters: $\lambda = 830$ nm; $w_x = 20$ mm; $w_y = 40$ mm; $r = 30$ mm; $z = 361{,}44$ m (3 Fresnel zones).

means, when Bessel functions are used, one can not use an ellipticaly symmetrical beam. In some applications, when rotationaly symmetrical beam is needed, or easily obtained, this restriction is fulfilled.

Derivation of equation comes from the integral 2.11, where for radius of diffrac-
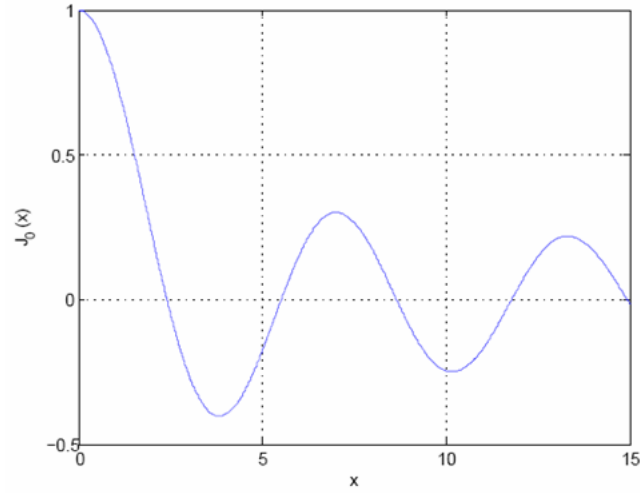
Fig. 4.2: Plot of Bessel function $J_0(x)$ of the first kind for order $\nu = 0$.

tion aperture a and planar wave with constant amplitude distribution applies

$$\psi_0(x_M, y_M) = \text{circ}\left(\frac{\rho_0}{a}\right). \tag{4.14}$$
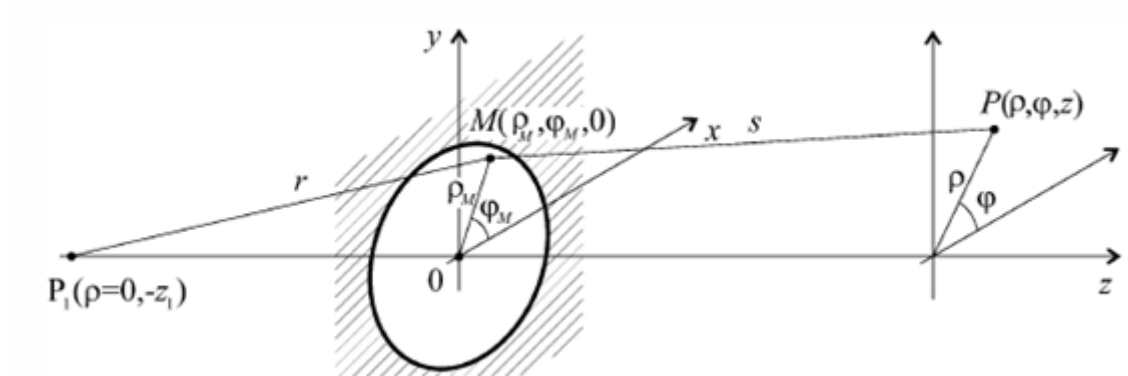
Fig. 4.3: Geometrical setup for rotationaly symmetrical case of Fresnel diffraction on circular aperture in an opaque shield. [1]

One has to transform s_M to cylindrical coordinates according to

$$s_M^2 = \rho_M^2 + \rho^2 - 2\rho_M\rho\cos(\varphi_M - \varphi) + z^2. \tag{4.15}$$

Meaning of symbols is obvious from figure 4.3. Then

$$\frac{\exp(jks_M)}{s_M} = \frac{\exp\left[jk\left(z + \frac{\rho^2}{2z}\right)\right]}{z}\exp\left\{\frac{jk}{2z}\left[\rho_M^2 - 2\rho_M\rho\cos\left(\varphi_M - \varphi\right)\right]\right\}. \tag{4.16}$$

Finaly can be equation 2.11 in cylindrical coordinates expressed in form

$$\psi(P) = -\frac{\mathrm{j}k}{2z} \frac{\exp\left[\mathrm{j}k\left(z + \frac{\rho^2}{2z}\right)\right]}{z} \int\limits_0^a \exp\left(\frac{\mathrm{j}k}{2z}\rho^2\right) \int\limits_0^{2\pi} \exp\left[-\frac{\mathrm{j}k}{z}\rho_M\rho\cos\left(\varphi_M - \varphi\right)\right]\mathrm{d}\varphi\rho\mathrm{d}\rho,$$

(4.17)

where inner integral can be expressed as Bessel function of the first kind as

$$\int\limits_0^{2\pi} \exp\left[-\frac{\mathrm{j}k}{z}\rho_M\rho\cos\left(\varphi_M - \varphi\right)\right]\mathrm{d}\varphi = 2\pi J_0\left(k\frac{\rho}{z}\rho_M\right).$$

(4.18)

Applying additional substitutions according to [1] leads to

$$\psi(\rho, z) = -\mathrm{j}2\pi n \exp\left[\mathrm{j}\left(kz + \pi\rho r^2\right)\right] \int\limits_0^1 \exp\left(\mathrm{j}\pi n t^2\right) J_0 2\pi n\rho t \mathrm{d}t.$$

(4.19)

For desired intensity applies

$$\psi\psi*(\rho) = (2\pi n)^2 \left\{ \left[\int\limits_0^1 \cos(\pi n t^2) J_0(2\pi n\rho t) t \mathrm{d}t\right]^2 + \left[\int\limits_0^1 \sin(\pi n t^2) J_0(2\pi n\rho t) t \mathrm{d}t\right]^2 \right\},$$

(4.20)

where n is number of observed Fresnel zones and ρ is distance from the axis of symmetry on the plane of receiver in the multiples of aperture radius a.

Expression 4.20 was finaly used as fundamental during development of programme simulating rotationaly symmetrical case of Fresnel diffraction on circular aperture.

In the script, there are multiple parameters to be defined, e.g. resolution res determines number of points in the graph, parameter rho_max determines maximal value on the x-axis to be displayed in the units of aperture radius and number of Fresnel zones n, that is determined by distance and wavelength according to equation 2.10. Recommended setting is $rho\_max = 1, 3$.

Script after being started numerically computes both integrals from the equation 4.20 and in cycle evaluates individual points of diffraction pattern. Output of the script are individual graphs for specified number of Fresnel zones - default value is $n \in\ < 1, 4 >$, i.e. first 4 Fresnel zones.
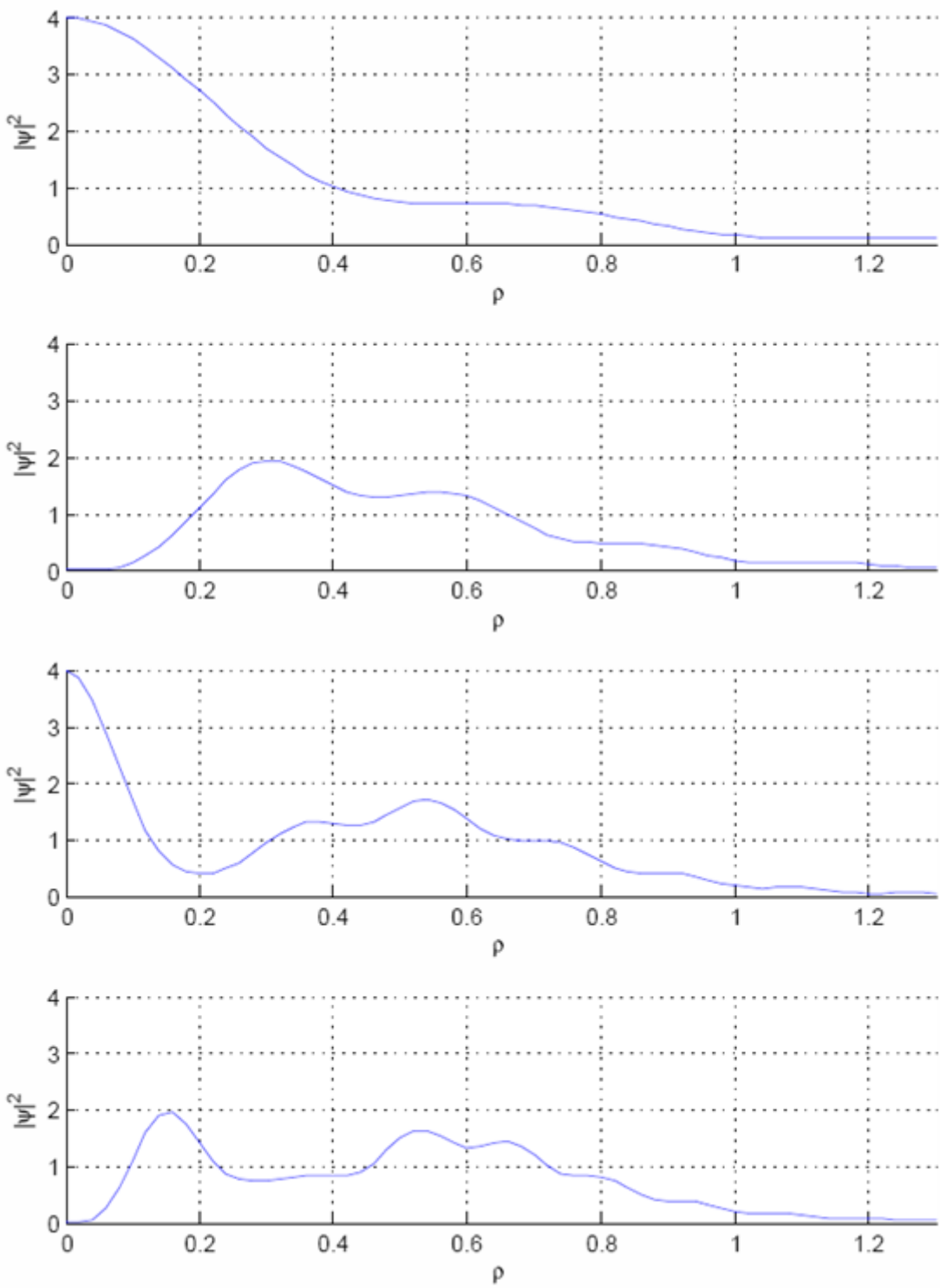
Fig. 4.4: Results of simulation using MATLAB script based on integration of Bessel functions. From top to the bottom: 1 to 4 Fresnel zones subsequently.

5 EXPERIMENT

In the previous text theoretical aspects of diffraction were introduced followed by practical realization of simulation. Although, results of both simulations had verified experimental experience, they were compared with a special experiment. The requirement for the experiment was physical accuracy.

5.1 Experimental prerequisities

Firstly, equation 2.14 applies for beam with one mode. Then, to prove function of the second model based on diffraction of Fresnel integral, the distribution of the intensity must be circularly symmetrical. Together with conditions introduced in section 4.1, there are following conditions to be fulfilled:

- Spatial coherence
- Time coherence
- Planar wave
- Circularly symmetrical distribution of intensity - constant or Gaussian
- Single-mode distribution of radiation

First two conditions are considered as fulfiled, as it was discussed in subsection 4.1.1. Planar distribution of phase in the plane of diffraction shield according to the third condition is not fulfilled when naked beam is considered. The beam from the laser must be collimated, i.e. placed to focus point of the lens very precisely. The rough setting can be carried out using simple method comparing the diameter of the beam spot in several distances from the lens. This diameter should not change along the distance. Then, more precise method should be used to finely set the distance of the lens from the laser to obtain planar wave on its output. For collimation planconvex lenses are practicaly used (see [6]), when the input laser beam is faced to the planar side of the lens to obtain the best result. Then, He-Ne laser is used for its relatively clean beam spot, i.e. small number of modes and its circularly symmetrical beam. Finaly, to acquire single-mode distribution of the beam, limiting-mode circular-hole diaphragm may be used. This device consists of microscope objective and circular-hole diaphragm and is used to supress higher modes of radiated laser beam by first magnifying the beam by the factor k and then placing a diaphragm of a diameter D approximately few microns to take single mode of the beam only.

5.2 Experimental layout

To satisfy all conditions mentioned above, following experimental layout was proposed:

- He-Ne laser ($\lambda = 632.8$ nm or $\lambda = 543.5$ nm)
- Modulator $f_{\mathrm{mod}} = 1$ kHz (Disc driven by motor designed to on-off keying of laser beam)
- Limiting-mode diaphragm consisting of
  - Objective $k = 25\times$
  - Diaphragm $D = 15~\mu$m
- Planconvex lens
  - Focal length $f = 0.3$ m
  - Diameter $D = 0.15$ m
- Shield with set of apertures with radius $r = 4$ mm and $r = 2.5$ mm
- Receiving photodiode
- Digital camera Nikon D90 with CCD chip (23.6×15.8) mm

The proposed layout was realised according to figure 5.1 and its part is shown on figure 5.2
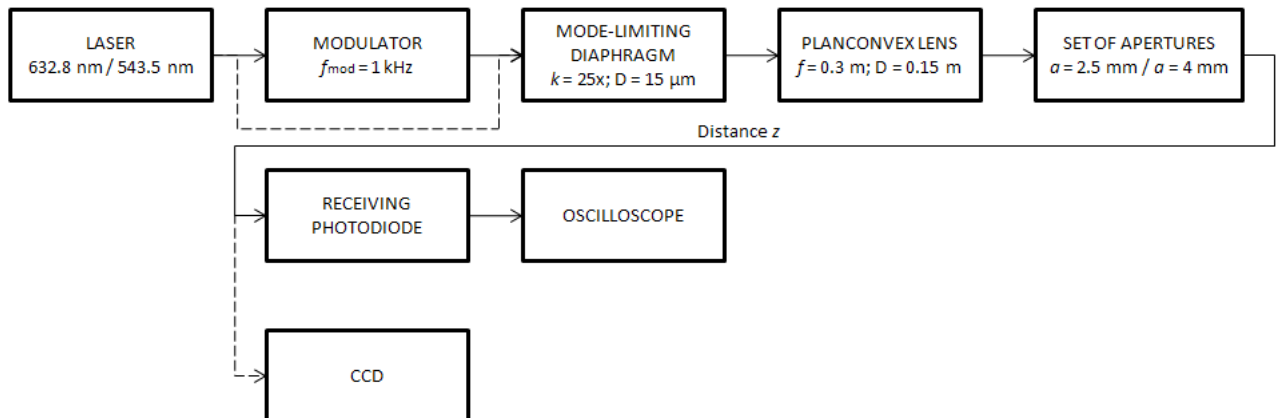
Fig. 5.1: Block diagram of the experiment. Alternative measurement with CCD chip is shown with dashed line.

The laser beam was directed through mechanical modulator to mode-limiting diaphragm. Single-mode beam was then collimated using planconvex lens. The collimation was crucial to obtain correct results, so it was carried out with maximum caution according to [6] using plane-parallel plate. To achieve good accuracy, micrometer shift drive in z-axis was used. Also, the best results are obtained when the lens faces its planar side to the beam. This setting produces single-mode planar laser beam that is assumed in all approximations mentioned in the text above.

Behind the lens, there is set of apertures. Plane of the aperture strip is referred above as plane of diffraction aperture. Then, in the distance z there is observation plane. In this case it is plane of receiving photodiode or CCD chip.

The photodiode is integrating the received signal from its whole surface. As one needs to render relatively small (few milimeters radius) spot with all its details, there is need for diaphragm to reduce the spot on the photodiode. For practical applications, black paper with a very small aperture made with a needle is sufficient. After placing the receivers' diaphragm to the center of the diffraction pattern, using the micrometer shift drive in x-axis and oscilloscope, values in the tables 5.1 to 5.8 in the following text were measured. These values were compared with values calculated using simulations introduced in the section 4.2.

Measurement using photodiode gives us accurate, but only one-dimensional behaviour of the pattern on the observation plane. To obtain two-dimensional distribution of the diffraction pattern, digital camera with CCD chip may be used. This measurement is marked in the figure 5.1 with dashed line. For this measurement, there was no photographic objective used. Pattern was recorded directly on the CCD chip.

Experiment was carried out for all combinations of
- Wavelength $\lambda = 632.8$ nm and $\lambda = 543.5$ nm
- Radius of diffraction aperture $r = 4.0$ mm and $r = 2.5$ mm
- Number of Fresnel zones $n = 3$ and $n = 4$, related to distance z according to equation 2.10

In the following text, results of simulations and experiment are presented and compared. Every measurement is introduced by title, with the set of parameters. First, there is MATLAB GUI simulating diffraction using FFT algorithm. Then, photograph of the diffraction pattern is showed followed by the table of distribution measured with photodiode. Finally, distribution measured with photodiode (black crosses) is compared with values calculated with script using FFT algorithm (red crosses) and script using integral of Bessel function (blue crosses).

5.3   Accuracy of results

In this section, deviations of measured values from simulated ones are mentioned. Main sources of uncertainty and deviation are determined and their impact on results of experiment are discussed.

- Setting of collimation
- Accuracy of determination of distance z from plane of diffraction aperture to observation plane
- Mechanical inaccuracy of the diffraction aperture
- Uncertainty in reading measured values of voltage on receiving photodiode on oscilloscope

Setting of collimation in the z-axis is crucial to obtain accurate results. As was experimentaly confirmed, change of lens position in z axis for approximately 3 mm resulted in qualitatively different pattern on observation plane, e.g. when collimated beam was set, there were 3 Fresnel zones observed on observation plane, but when the lens was moved in z-axis for 3 mm, there were 4 Fresnel zones observed. Quantitaively, applying used lens with focus length $f = 0.3$ m, deviation of only 1% resulted in qualitatively different pattern on observation plane. Its greatest impact is for values near the axis $0z$, i.e. axis of symmetry for rotationally symmetrical systems like the one in experiment. Practically, the collimation can be set with an accuracy of determination of distance of lens from laser $\Delta z_1 = 0.5$ mm for $f = 0.3$ m and accuracy of collimation $\delta_c = 0.2$ % can be achieved.

Accuracy of determination of distance z is critical especially for distances in Fresnel region, i.e. distances smaller then Rayleigh distance z_0. It is given according to the equation 2.10 and it can be seen, that change in the distance has impact on the diffraction pattern as the Fresnel number N_f is determined by the distance z. In the experiment, accuracy of placing the detector to determined distance was approximately $\Delta z = 3$ cm for distances of order of metres. That results in accuracy of $\delta_z = 0.5$ %. It was difficult to determine distance z for taking a photograph with digital camera. The camera that was used in experiment has set of mirrors and it was not known what distance does the beam inside the camera travels. Reasonable estimation of accuracy for determination of distance z for experiment with camera was $\Delta z = 10$ cm, that resulted in accuracy $\delta_z = 1.5$ %.

The set of aperture was made of epoxide with thickness $h = 2$ mm by electrical drill with a standard set of drills. The accuracy of the size is approximately $\Delta a = 0.05$ mm, i.e. $\delta_a = 1.25$ % for aperture with $a = 4$ mm. Change of the aperture diameter in this order may be noticable and may cause disagreement between simulation and experiment. According to the simulations, the difference would not be qualitative, but may cause change in the shape of second maxima in case three or four Fresnel zones are observed.

According to the experimental layout, results were observed with photodiode detector. Therefore, the laser beam must have been modulated with $f_{\mathrm{mod}} = 1$ kHz. This allowed to observe the voltage signal on oscilloscope and using cursors, determine its peak-to-peak value. Signal on the photodiode is relatively small and

producing output voltage in order of tens of milivolts. Additionaly, the signal was, especially for the laser with $\lambda = 543.5$ nm, noisy and causing higher deviation of reading of values. The accuracy was estimated as $\delta V_{pp} = 5$ %.

Error of setting the small aperture of photodiode should also be considered. It should have diameter greater than the step of measurement in x-axis. This statement is considered to be fullfiled. There is an error related to the position of this aperture in the y-axis. It should be placed precisely on the vertical axism otherwise it will cause additional error when there is not sharp maximum or minimum in the origin and also the measured pattern would be proportionaly smaller with respect to the simulated pattern.

Summing all deviations mentioned in the text above results in estimation of overall deviation estimation

$$\delta_{meas} = \delta_c + \delta_z + \delta_a + \delta V_{pp} = 0.2 + 0.5 + 1.25 + 5 = 7.95\%. \tag{5.1}$$

This error was considered in results simulated using FFT to determine area in which should measured results fall into and this area was displayed in graphs below.
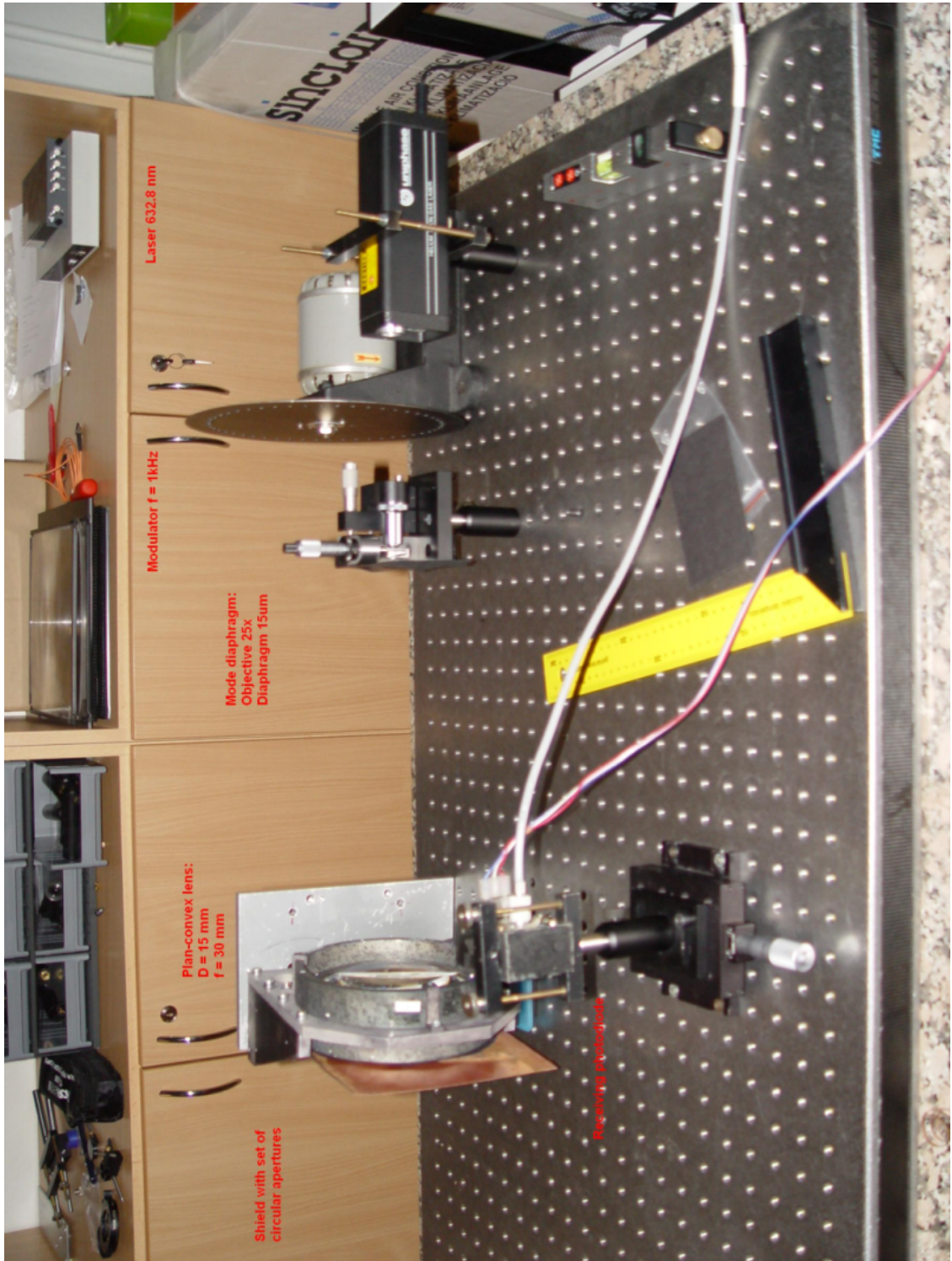
Fig. 5.2: Realisation of the experiment.

Parameters of simulation: $\lambda = 632.8$ **nm;** $a = 4.0$ **mm;** $z = 8.43$ **m;** $n = 3$

Fig. 5.3: Simulation of Fresnel diffraction using model based on FFT.
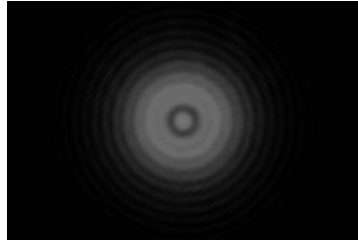
Fig. 5.4: Digital photograph of simulated diffraction pattern on CCD chip.

x [mm]	12.60	12.80	13.00	13.20	13.40	13.60	13.80	14.00	14.20	14.40
V_{pp}[mV]	218.8	165.6	85.63	39.06	27.66	38.44	63.44	82.50	82.50	91.88
x [mm]	14.60	14.80	15.00	15.20	15.40	15.60	15.80	16.00	16.20	16.40
V_{pp}[mV]	97.50	97.50	70.31	52.19	49.06	42.50	29.53	27.97	27.97	20.94
x [mm]	16.60	16.80	17.00	17.20	17.40	17.60	17.80	18.00		
V_{pp}[mV]	12.81	10.25	7.812	3.688	2.438	3.00	2.00	1.50		

Tab. 5.1: Measured voltage on receiving photodiode using oscilloscope.

Fig. 5.5: Comparison of both models (red - FFT, blue - Bessel function integration) with measured diffraction pattern distribution (black).

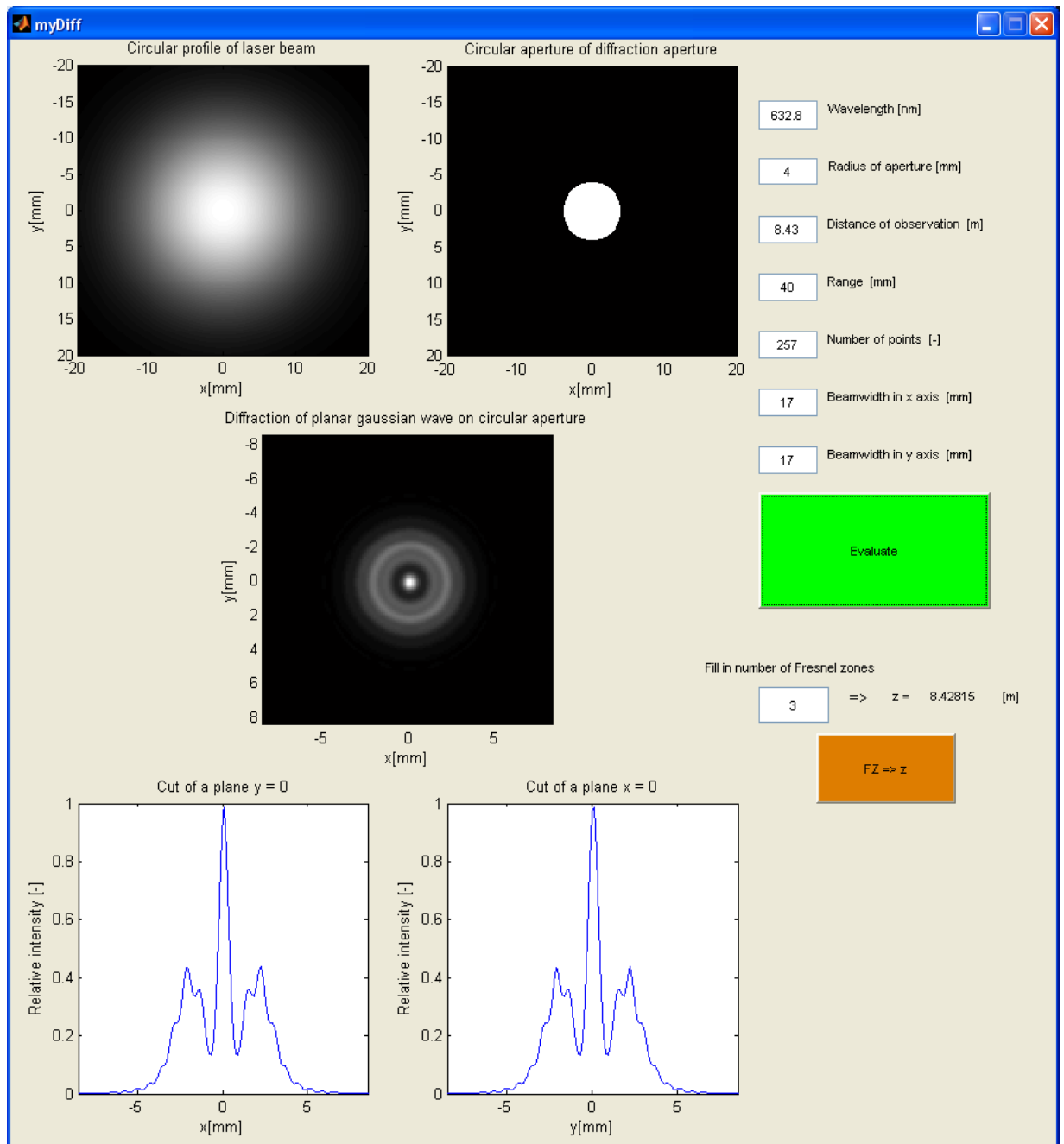**Parameters of simulation:** $\lambda = 632.8$ **nm;** $a = 4.0$ **mm;** $z = 6.32$ **m;** $n = 4$

Fig. 5.6: Simulation of Fresnel diffraction using model based on FFT.
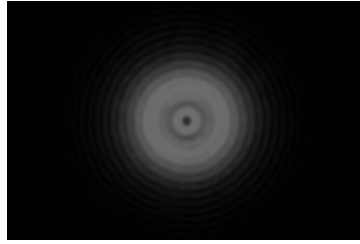
Fig. 5.7: Digital photograph of simulated diffraction pattern on CCD chip.

x [mm]	4.75	4.90	5.00	5.10	5.20	5.40	5.60	5.80	5.90	6.00	6.10
V_{pp}[mV]	7.875	15.78	35.94	63.13	86.88	100.00	95.00	55.94	45.63	41.56	41.87
x [mm]	6.20	6.40	6.60	6.80	7.00	7.20	7.40	7.60	7.80	8.00	8.20
V_{pp}[mV]	43.75	47.19	51.88	60.62	71.87	63.75	63.75	68.75	54.69	49.06	43.13
x [mm]	8.40	8.60	8.80	9.00	9.20	9.40	9.60	9.80	10.00		
V_{pp}[mV]	27.50	21.09	12.69	6.188	6.875	4.750	3.938	3.562	2.000		

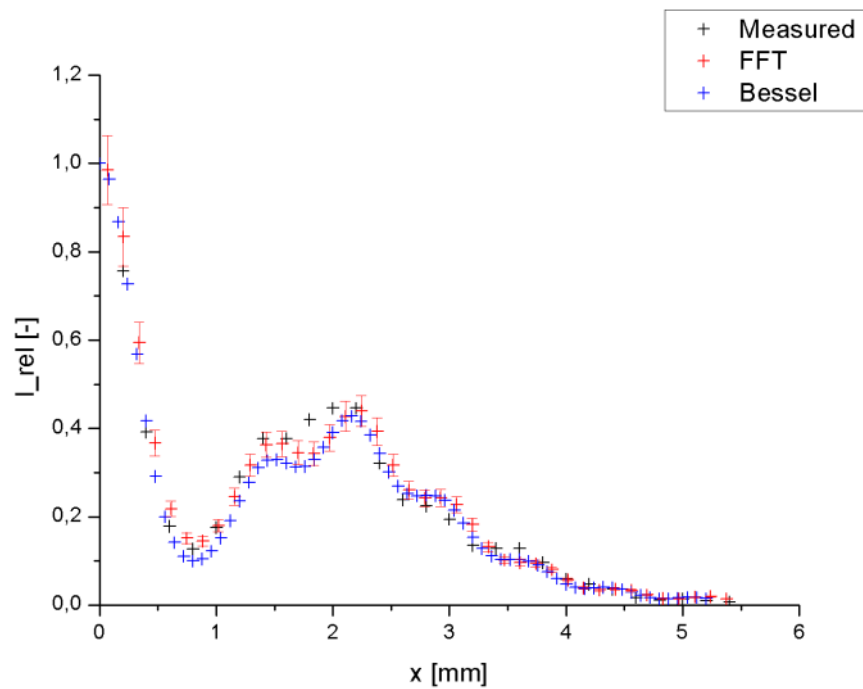Tab. 5.2: Measured voltage on receiving photodiode using oscilloscope.

Fig. 5.8: Comparison of both models (red - FFT, blue - Bessel function integration) with measured diffraction pattern distribution (black).

42

Parameters of simulation: $\lambda = 632.8$ **nm;** $a = 2.5$ **mm;** $z = 3.29$ **m;** $n = 3$
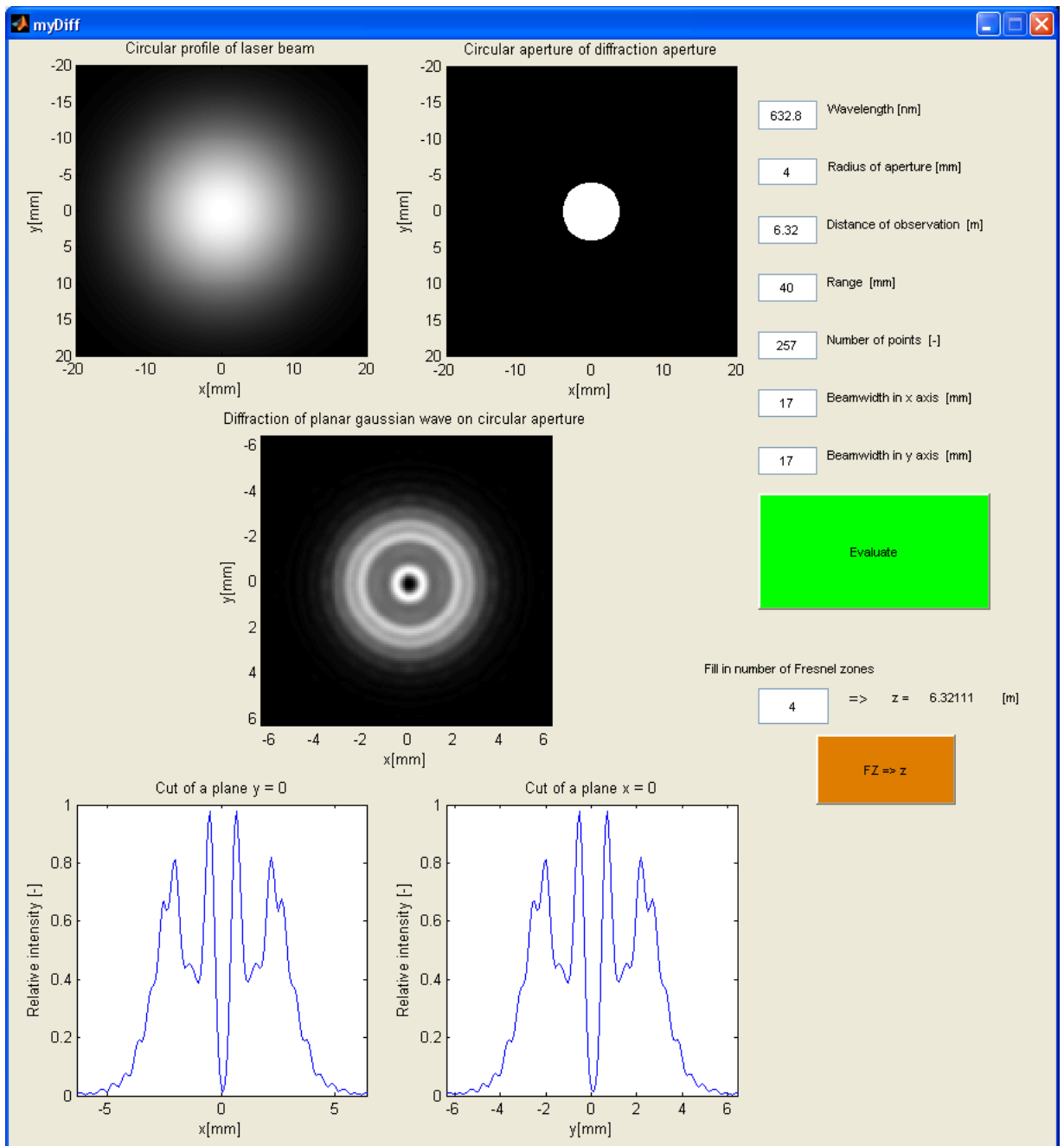

Fig. 5.9: Simulation of Fresnel diffraction using model based on FFT.
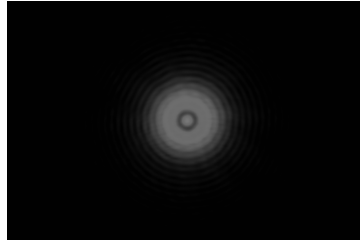
Fig. 5.10: Digital photograph of simulated diffraction pattern on CCD chip.

x [mm]	7.55	7.70	7.80	7.90	8.00	8.10	8.20	8.30	8.40
V_{pp}[mV]	92.50	61.56	34.7	16.25	9.625	10.75	17.19	28.59	37.50
x [mm]	8.50	8.60	8.70	8.80	8.90	9.00	9.10	9.20	9.30
V_{pp}[mV]	40.94	38.44	36.25	36.25	36.56	33.13	26.41	22.03	22.34
x [mm]	9.40	9.50	9.60	9.70	9.80	9.90	10.00	10.10	10.20
V_{pp}[mV]	22.97	19.37	13.63	9.688	8.313	7.000	5.188	3.500	3.310

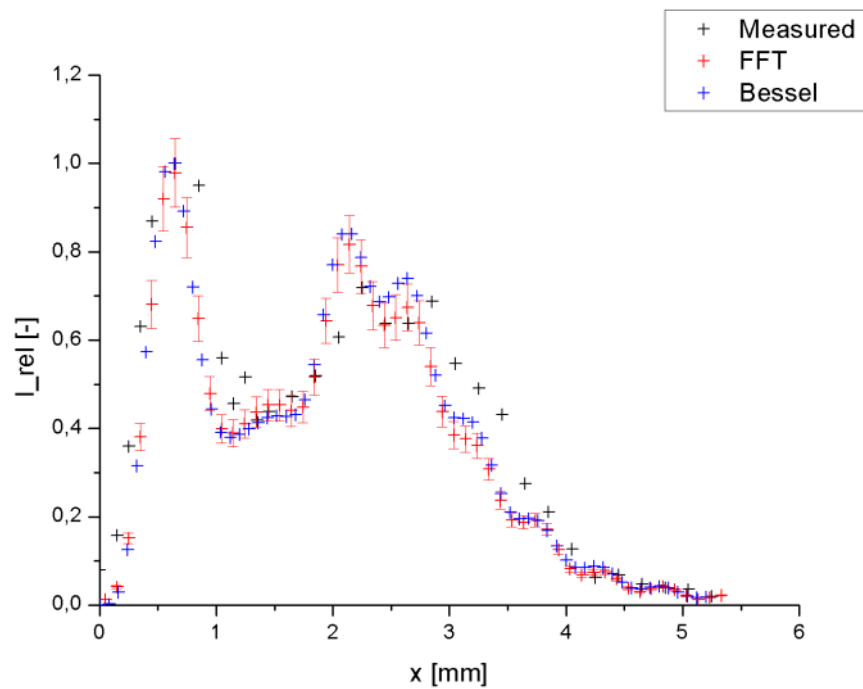Tab. 5.3: Measured voltage on receiving photodiode using oscilloscope.

Fig. 5.11: Comparison of both models (red - FFT, blue - Bessel function integration) with measured diffraction pattern distribution (black).

44

Parameters of simulation: $\lambda = 632.8$ **nm;** $a = 2.5$ **mm;** $z = 2.47$ **m;** $n = 4$
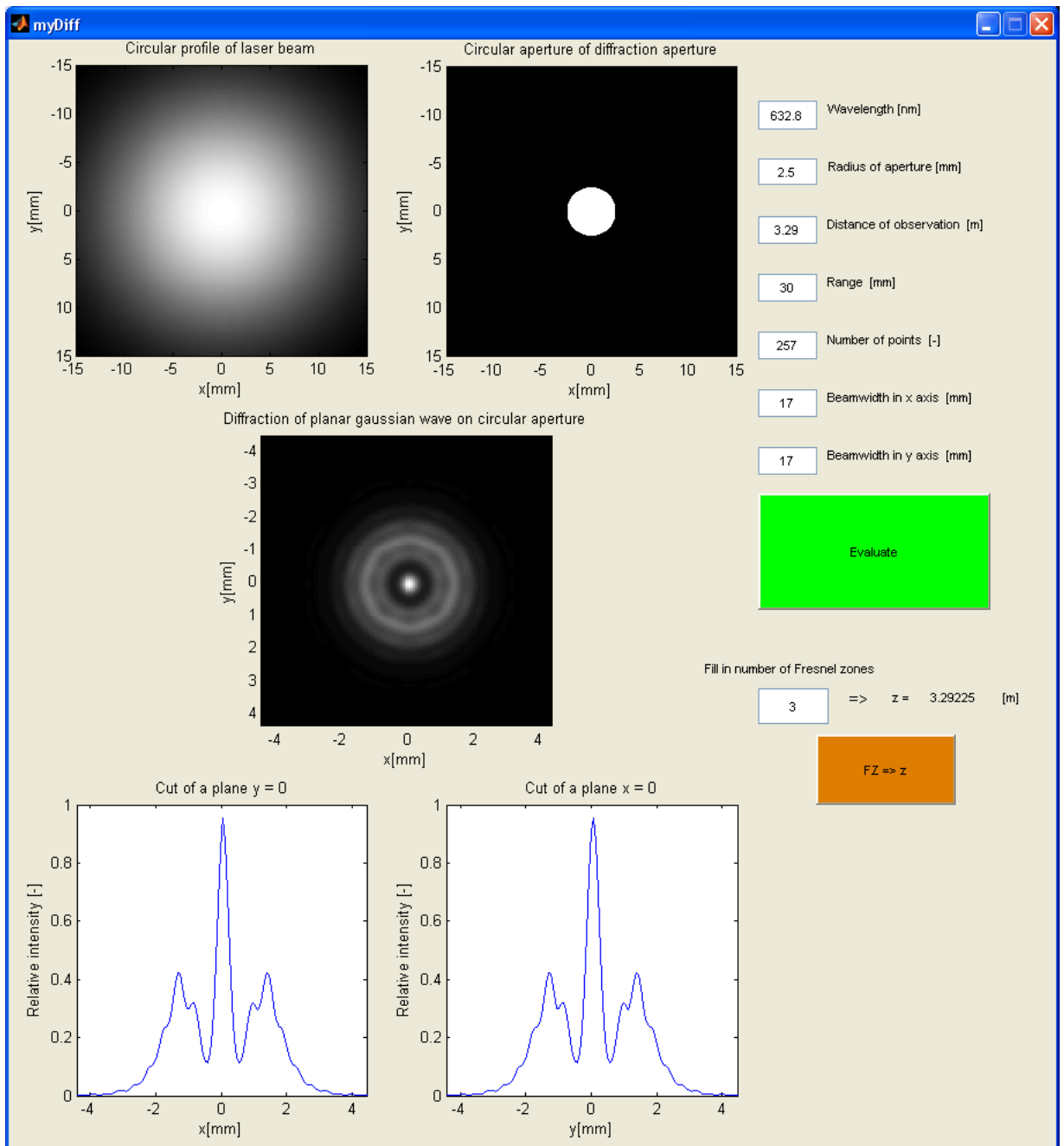

Fig. 5.12: Simulation of Fresnel diffraction using model based on FFT.
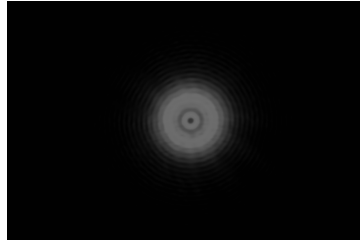
Fig. 5.13: Digital photograph of simulated diffraction pattern on CCD chip.

x [mm]	14.15	14.30	14.40	14.50	14.60	14.70	14.80	14.90	15.00
V_{pp}[mV]	3.188	12.38	29.06	39.69	32.19	17.97	10.63	9.688	12.31
x [mm]	15.10	15.20	15.30	15.40	15.50	15.60	15.70	15.80	15.90
V_{pp}[mV]	15.16	16.87	20.63	28.44	31.88	28.44	23.59	20.94	18.59
x [mm]	16.00	16.10	16.20	16.30	16.40	16.50	16.60	16.70	16.80
V_{pp}[mV]	14.19	13.69	12.75	9.75	6.062	5.437	4.813	3.437	3.000

Tab. 5.4: Measured voltage on receiving photodiode using oscilloscope.
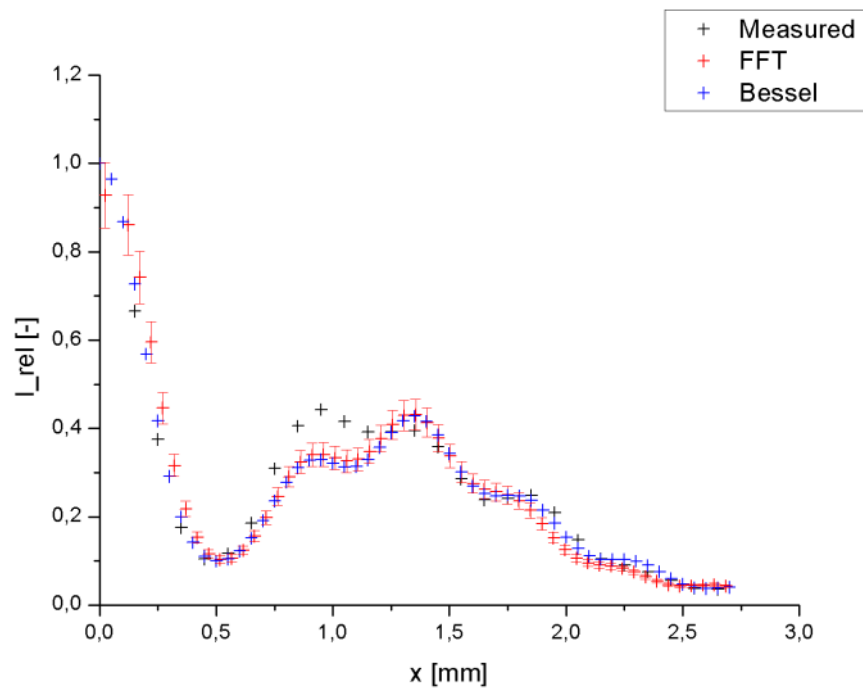

Fig. 5.14: Comparison of both models (red - FFT, blue - Bessel function integration) with measured diffraction pattern distribution (black).

46

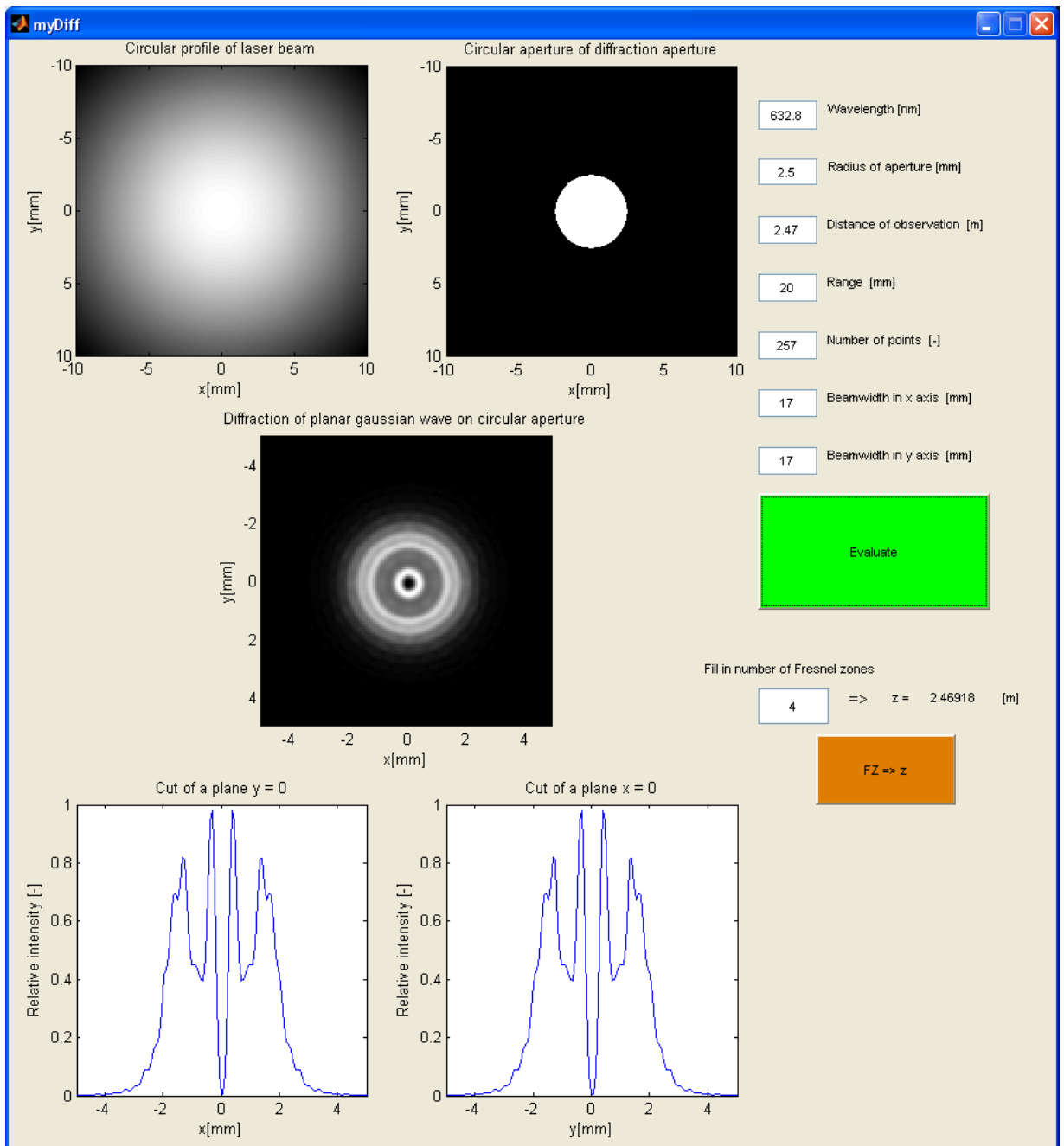**Parameters of simulation:** $\lambda = 543.5$ **nm;** $a = 4.0$ **mm;** $z = 9.81$ **m;** $n = 3$

Fig. 5.15: Simulation of Fresnel diffraction using model based on FFT.
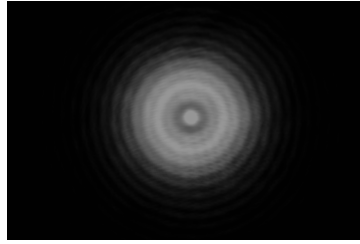
Fig. 5.16: Digital photograph of simulated diffraction pattern on CCD chip.

x [mm]	5.15	5.30	5.50	5.70	5.90	6.00	6.10	6.30	6.50
V_{pp}[mV]	125	113.1	65.62	35.16	25.47	25.00	25.47	33.44	39.38
x [mm]	6.70	6.90	7.10	7.30	7.50	7.70	7.90	8.10	8.30
V_{pp}[mV]	39.38	44.06	60.94	65.31	48.75	40.00	39.06	35.63	24.69
x [mm]	8.50	8.70	8.90	9.10	9.30	9.50	9.70		
V_{pp}[mV]	19.06	17.81	13.59	8.063	7.375	6.250	3.688		

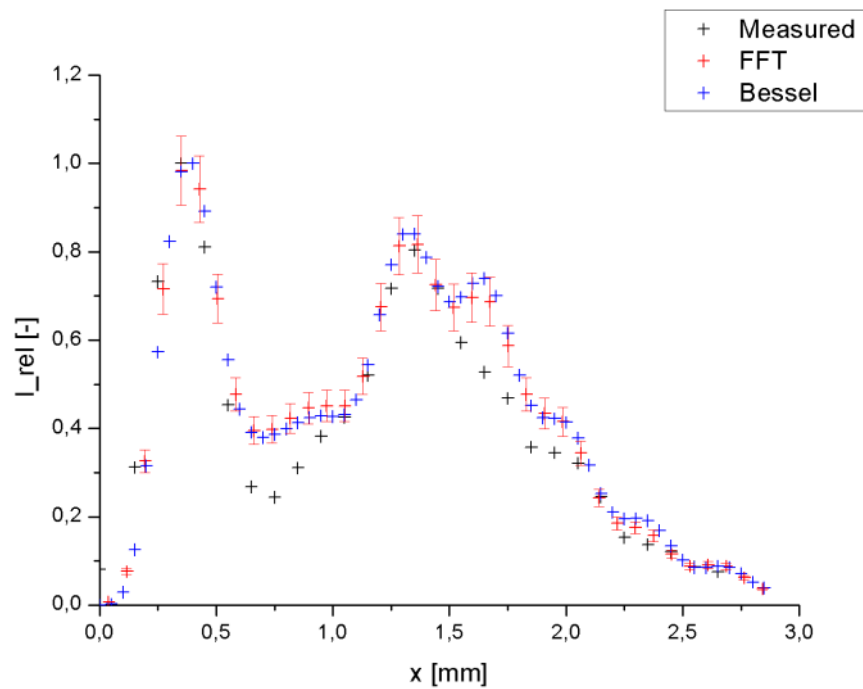Tab. 5.5: Measured voltage on receiving photodiode using oscilloscope.
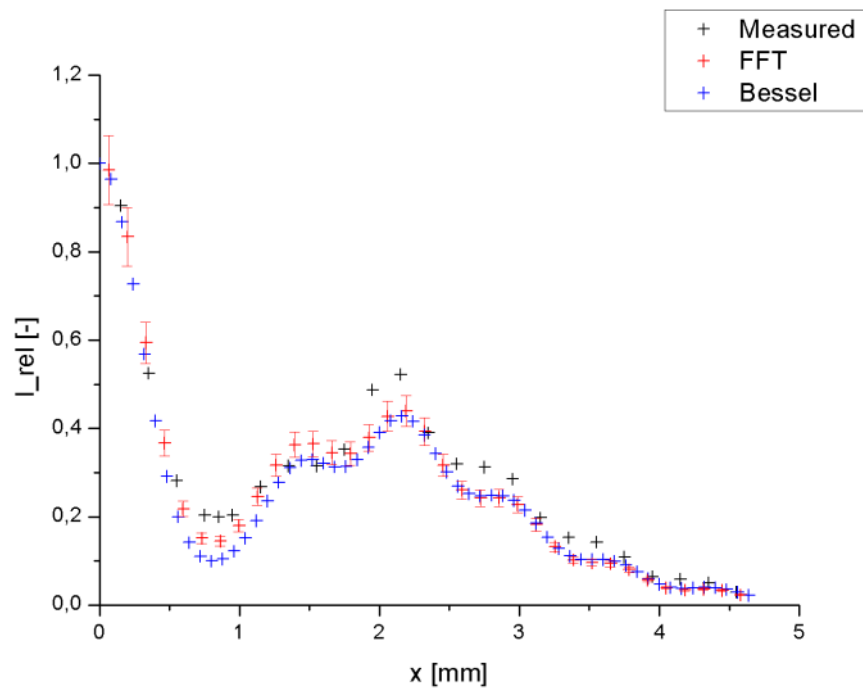
Fig. 5.17: Comparison of both models (red - FFT, blue - Bessel function integration) with measured diffraction pattern distribution (black).

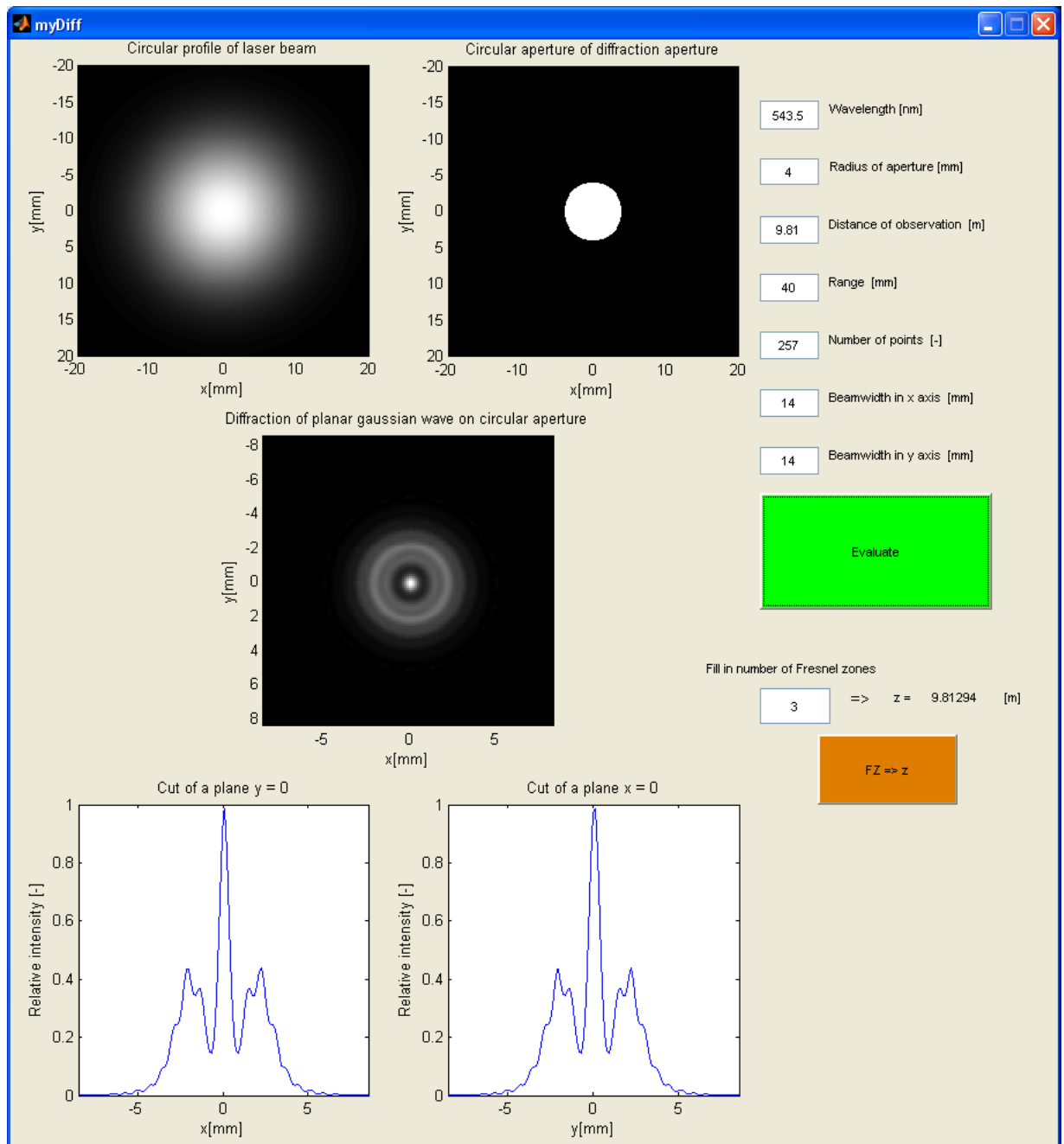**Parameters of simulation:** $\lambda = 543.5$ **nm;** $a = 4.0$ **mm;** $z = 7.36$ **m;** $n = 4$

Fig. 5.18: Simulation of Fresnel diffraction using model based on FFT.
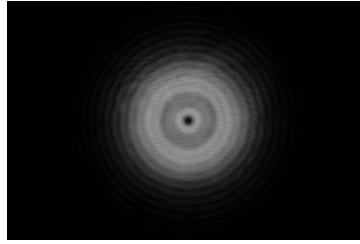
Fig. 5.19: Digital photograph of simulated diffraction pattern on CCD chip.

x [mm]	9.65	9.80	9.90	10.00	10.10	10.20	10.30	10.40	10.50
V_{pp}[mV]	6.375	9.875	18.44	33.75	51.25	62.19	62.19	52.81	40.63
x [mm]	10.60	10.70	10.80	10.90	11.00	11.10	11.20	11.30	11.40
V_{pp}[mV]	30.16	23.59	22.34	24.53	26.87	28.91	31.72	31.72	30.31
x [mm]	11.50	11.60	11.70	11.80	11.90	12.00	12.10	12.20	12.40
V_{pp}[mV]	32.97	39.03	44.69	47.19	47.19	40.31	37.81	36.56	35.63
x [mm]	12.60	12.80	13.00	13.20	13.40	13.60	13.80	14.00	
V_{pp}[mV]	26.56	20.94	17.81	10.63	9.125	7.500	4.250	3.438	

Tab. 5.6: Measured voltage on receiving photodiode using oscilloscope.

Fig. 5.20: Comparison of both models (red - FFT, blue - Bessel function integration) with measured diffraction pattern distribution (black).

Parameters of simulation: $\lambda = 543.5$ **nm;** $a = 2.5$ **mm;** $z = 3.83$ **m;** $n = 3$
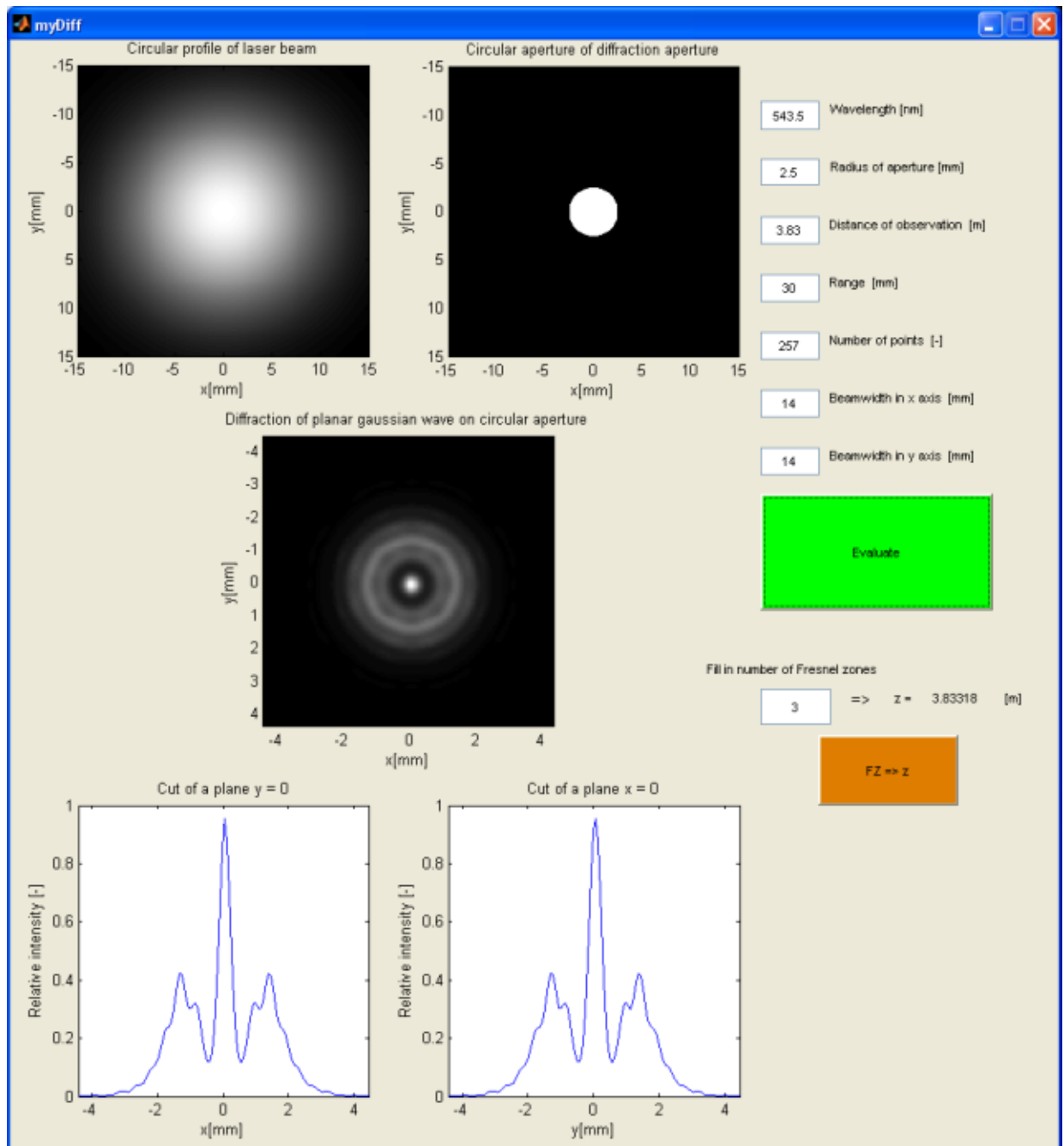
Fig. 5.21: Simulation of Fresnel diffraction using model based on FFT.
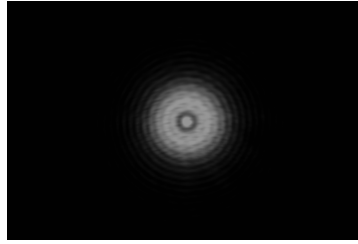
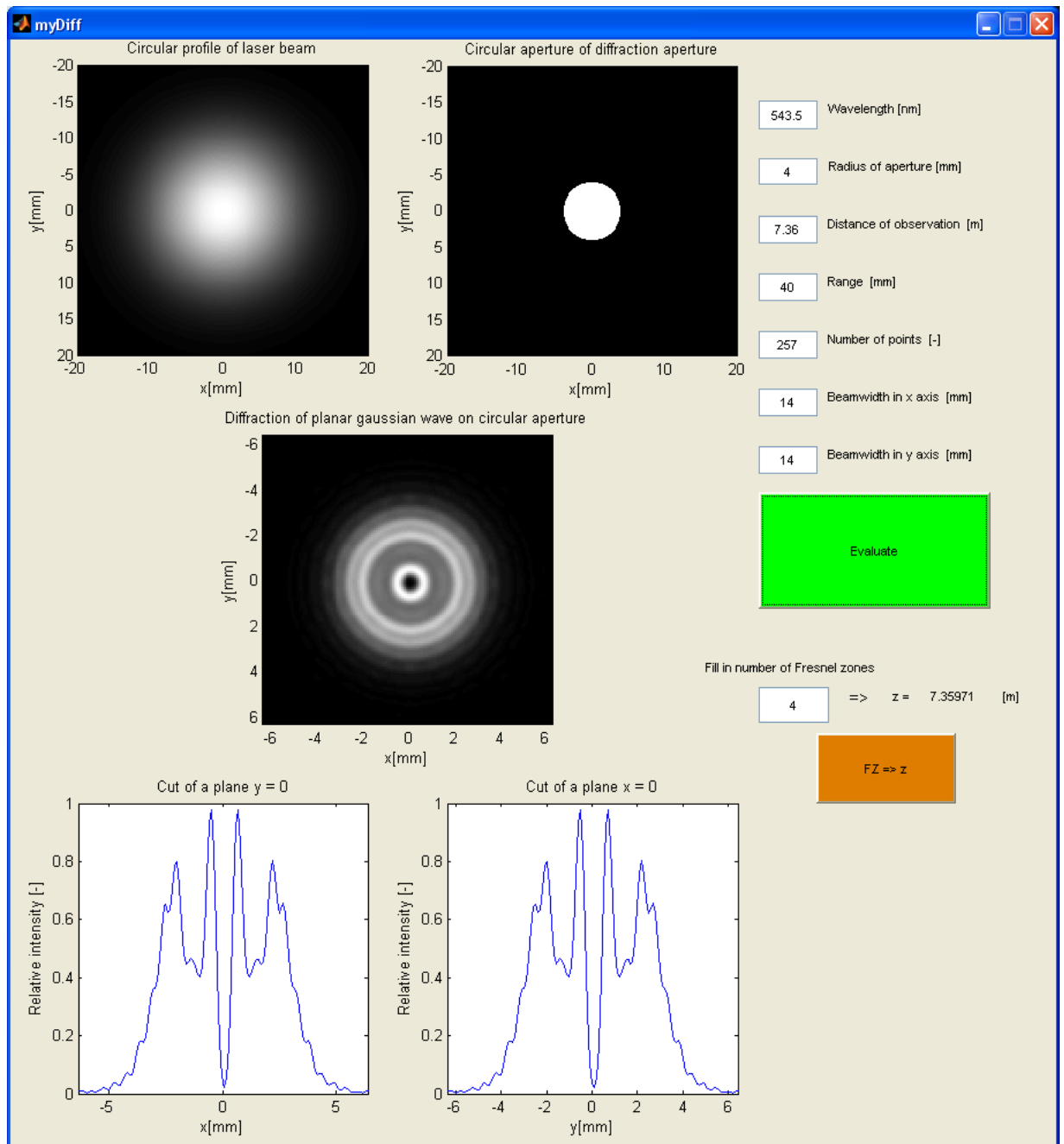Fig. 5.22: Digital photograph of simulated diffraction pattern on CCD chip.

x [mm]	9.35	9.40	9.50	9.60	9.70	9.80	9.90	10.00	10.10
V_{pp}[mV]	63.75	57.81	37.19	22.66	11.75	8.563	10.06	15.94	23.91
x [mm]	10.20	10.30	10.40	10.50	10.60	10.70	10.80	10.90	11.00
V_{pp}[mV]	29.38	29.53	26.87	25.94	29.06	28.44	25.94	18.75	16.09
x [mm]	11.10	11.20	11.30	11.40	11.50	11.60	11.70	11.80	11.90
V_{pp}[mV]	15.78	15.47	12.50	8.938	7.062	6.186	5.313	4.125	2.687

Tab. 5.7: Measured voltage on receiving photodiode using oscilloscope.
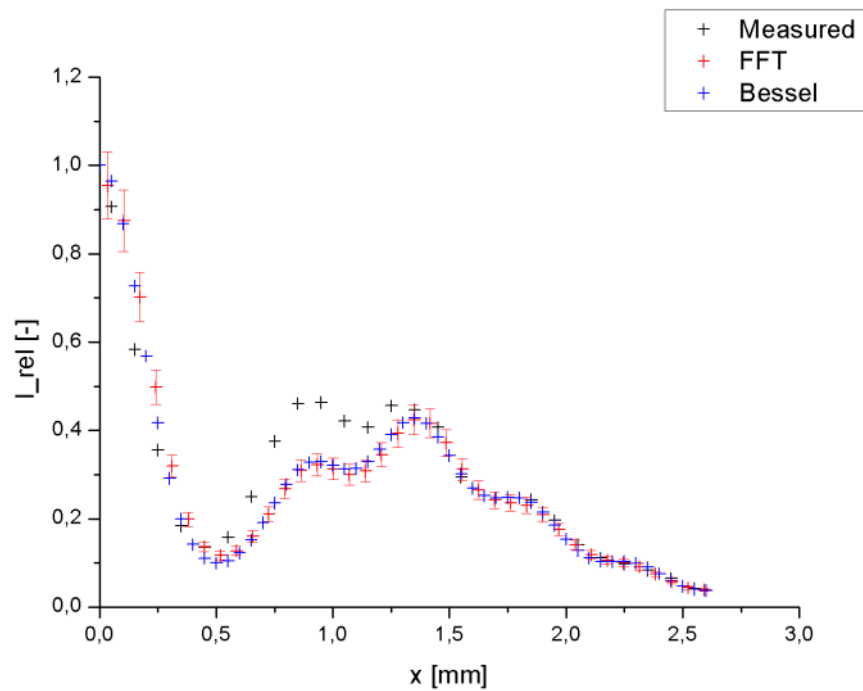
Fig. 5.23: Comparison of both models (red - FFT, blue - Bessel function integration) with measured diffraction pattern distribution (black).

Parameters of simulation: $\lambda = 543.5$ **nm;** $a = 2.5$ **mm;** $z = 2.87$ **m;** $n = 4$
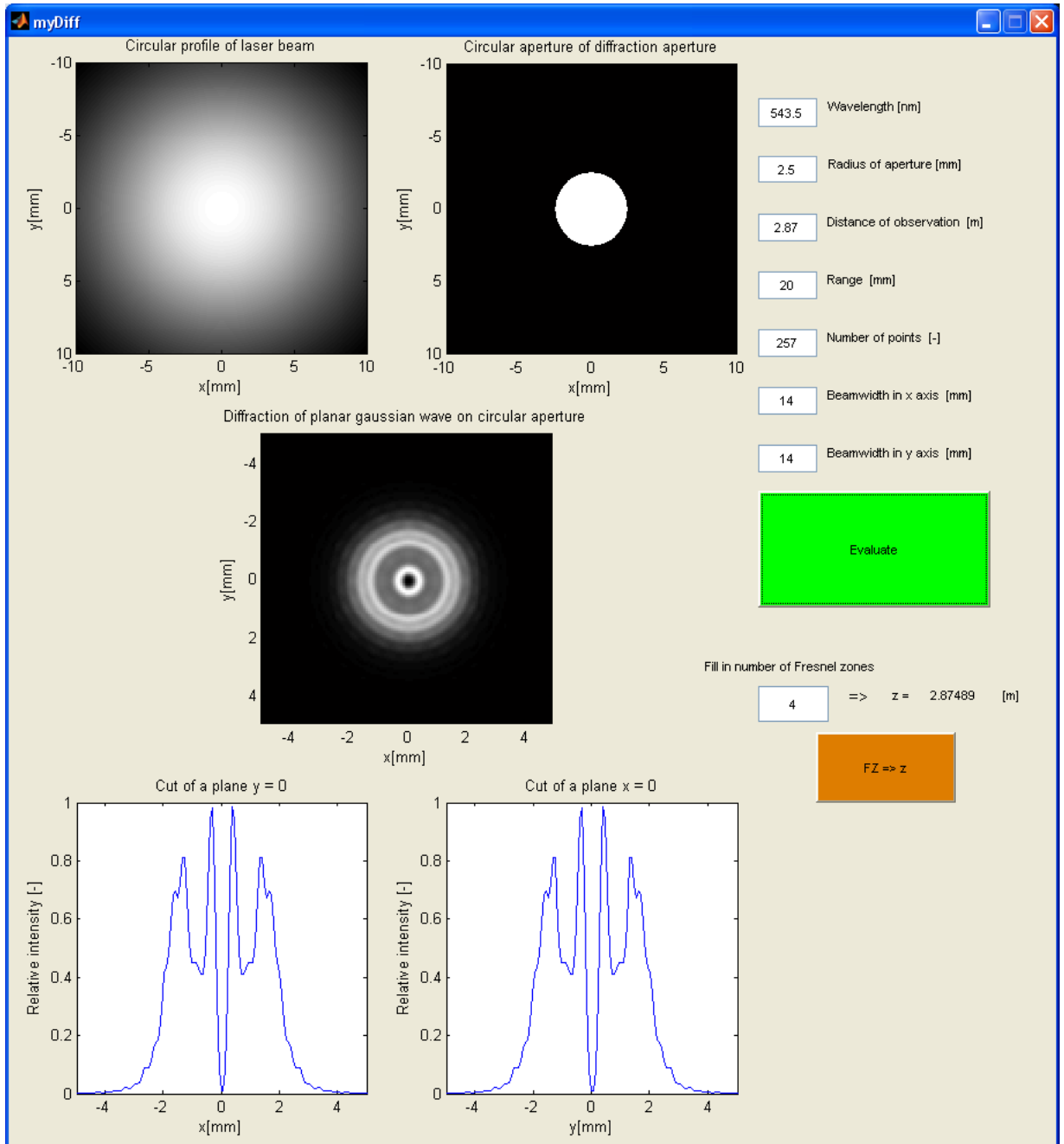
Fig. 5.24: Simulation of Fresnel diffraction using model based on FFT.
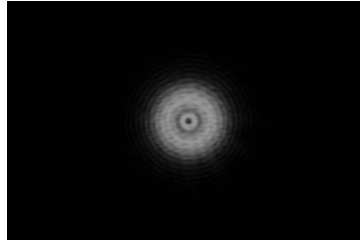
Fig. 5.25: Digital photograph of simulated diffraction pattern on CCD chip.

x [mm]	5.20	5.30	5.40	5.50	5.60	5.70	5.80	5.90	6.00
V_{pp}[mV]	3.75	5.813	12.50	20.78	21.25	15.47	9.875	7.875	8.938
x [mm]	6.10	6.20	6.30	6.40	6.50	6.60	6.70	6.80	6.90
V_{pp}[mV]	11.81	13.06	13.06	14.69	17.81	18.44	16.25	15.62	15.31
x [mm]	7.00	7.10	7.20	7.30	7.40	7.50	7.60	7.70	7.80
V_{pp}[mV]	12.00	9.50	8.125	6.875	4.687	3.75	3.75	3.00	2.06

Tab. 5.8: Measured voltage on receiving photodiode using oscilloscope.
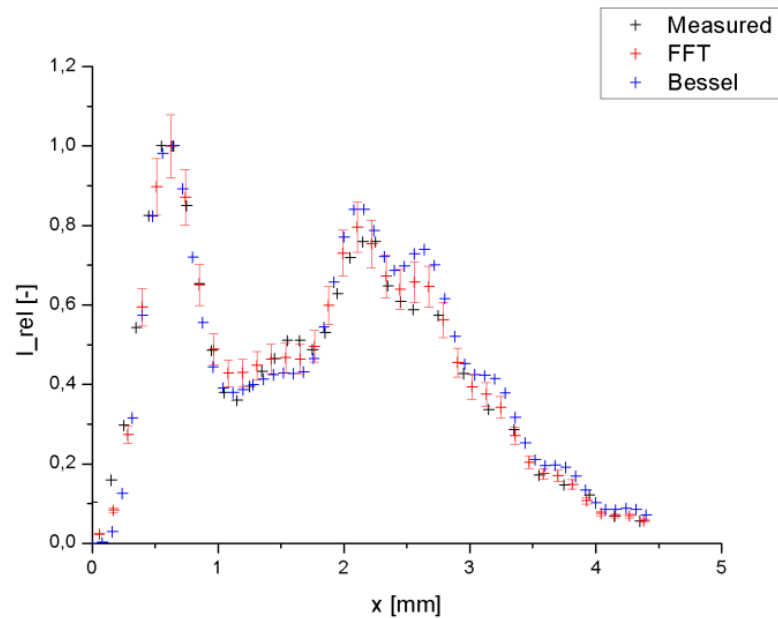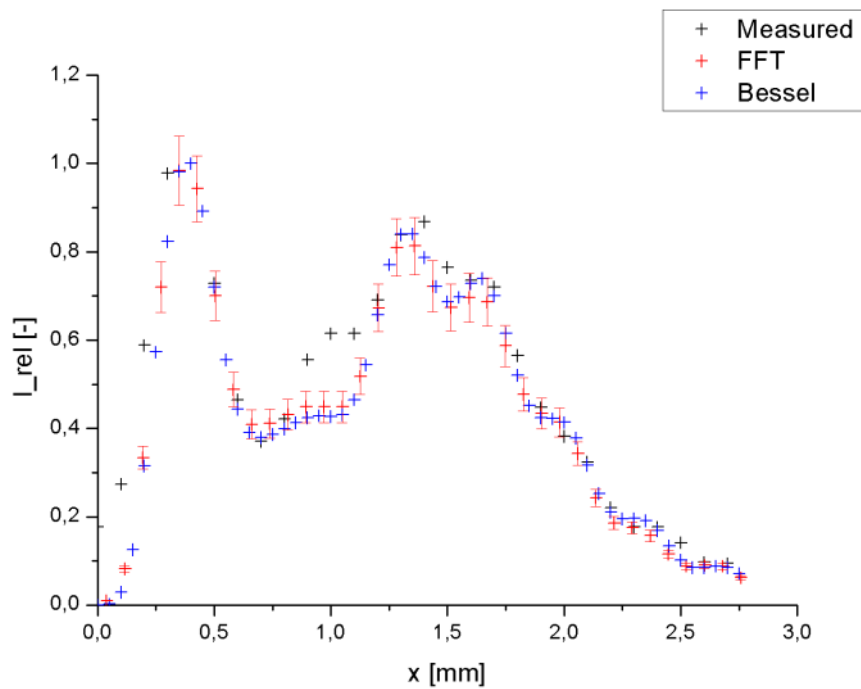

Fig. 5.26: Comparison of both models (red - FFT, blue - Bessel function integration) with measured diffraction pattern distribution (black).

6 DISCUSSION

In this chapter, results of both simulations and measurement according to the experiment introduced in chapter 5.2 are discussed.

6.1 Confrontation of the model with experiment

Both models presented in section 4.2 were compared and confronted with real experiment introduced in section 5.2. Results of this experiment displayed in graphs above matched expectations based on both simulations. This match is also statistically analysed according to estimation of deviation in section 5.3 and error bars were added to results of simulation based on FFT to determine area in which should theoretically the experimental results fall.

Further analysis shows that the deviation of the measured values is higher, because the overall deviation is not simply sum (see equation 5.1) of partial deviations caused by individual effects mentioned in section 5.3. For instance, 3 % change of the distance of lens from the laser will result in overall change of the diffraction pattern observed in distance z. Therefore to analyse precisely impact of partial deviations, estimation based on error propagation effect should be used. This method requires to solve partial derivative of function 2.14 with respect to all variables mentioned in the section 5.3.

6.2 How to estimate Fresnel number

Number of Fresnel zones of laser beam with wavelength λ observed in a given distance z and using given radius of aperture a is determined according to equation 2.20. As it is given precisely with a geometry of the system, it can provide valuable information. The Fresnel number can be seen directly from the diffraction pattern, however, it is not easy and it can lead to misjudge. As can be seen from photographs, there are multiple circles, that should not be included in Fresnel number estimation. The best way to determine how many Fresnel zones are observed is to measure distribution of intensity in a given distance and calculate according to contrast between local maxima and minima. Threshold between cases when include or not a maxima to Fresnel number estimation should be set empirically. Contrast can be calculated as follows

$$k = \frac{I_{\max} - I_{\min}}{I_{\max} + I_{\min}} \tag{6.1}$$

,

where I_{max} and I_{min} are relative intensity of maximum and minimum respectively. Reasonable estimation of threshold according to the simulation would be approximately $k = 0.5$, i.e. Fresnel zone can be calculated, when contrast between local maximum and minimum exceeds $k = 0.5$.

6.3   Geometrical and diffraction divergency

Geometrical divergency is determined by increase of beamwidth along the z-axis in the direction of propagation. This divergency is natural for all lasers. To meet the theoretical requirements, collimated beam was used in the experiment, i.e. beam with constant beamwidth along z-axis. This applies for first geometrical approximation of the beam.

Because of Heisenberg uncertainty principle the beam is always slightly divergent. It can be seen as well from the Huygens principle in the section 2.2, that the secondary waveform on the edge of the aperture causes additional divergency. This divergency is significant only when the beam is precisely collimated. Otherwise geometrical divergency exceeds the effect of diffraction divergency.

At this point, numerical estimation of this effect is important. For Gaussian beam divergency, evolution of beamwidth size along beam propagation is fundamental. Its difference divided by the distance is approximately equal to beam divergency. Distribution of diffraction pattern in Fresnel region can not be approximated by Gaussian distribution to apply the same metrics and determine divergency of the beam behind the aperture. However, one may use his own arbitrary method to determine the divergency.

One of the method would be based on the definition of divergency of the Gaussian beam and requires graphical representation of the intensity distribution (e.g. graph 5.9). The beamwidth of the diffraction pattern would be distance from the axis of symmetry to the point, where intensity of the pattern equals $I_0 e^{-2}$, where I_0 is maximum intensity in the diffraction pattern. The problem is, when more Fresnel zones are observed. Then, using this method, estimation of the beamwidth would be much smaller. In this case, one should start in the center of the diffraction pattern and going outwards, while counting number of Fresnel zones. When all of them are counted, going still outwards, one reaches the point in the graph, where the intensity equals desired level and takes this as the beamwidth. Then the procedure is same as for Gaussian beam.

6.4 Real consequences of Fresnel diffraction

First, one has to realize, when does Fresnel diffraction occurs. Standard systems for free-space optical communications have following parameters regarding diffraction effects: Wavelength $\lambda = 850$ nm and Radius of diffraction aperture (Lens holder clamp) $a = 25$ mm. In this case, range of Fresnel diffraction effects, i.e. range, where Fresnel number $N_f \geq 1$ is until the distance z_0, where $N_f = 1$ according to equation 2.20

$$z_0 = \frac{a^2}{\lambda} = \frac{(25.10^{-3})^2}{850.10^{-9}} = 735 \text{m}. \tag{6.2}$$

On the other hand, when Fresnel number raise above certain level, Fresnel zones are not distinguishable in the pattern. This occurs for distances much lower than z_0, e.g. $z(N_f = 20) = 37$ m.

Most of communication operate in distances less than z_0 above, but more, than threshold for 20 Fresnel zones and therefore, in the region, where Fresnel diffraction occurs. Diffraction and especially Fresnel diffraction brings limitations in practical applications.

Main concern regarding diffraction in optical communication is in PAT (pointing, acquisition and tracking) systems. These systems are used to precisely point the beam to the receiver's aperture. To achieve this, the receiver has to lock on the receiving beam. When in the plane of receiver more than one local maxima are observed, system may lose communication as they are not capable to distinguish on which to lock. Additionaly, these local maxima are narrower than beam propagating in the free space with no diffraction, so locking on the central maxima (when N_f is odd) is neither ideal solution.

One of the method to avoid diffraction is to use lens wider than beamwidth on the plane of collimation. Simulations and further experiments show, that using lens size comparable to beamwidth reduces diffraction effects significantly. For this purpose, ratio $\frac{w}{a}$ of beamwidth w to radius of lens a is defined. Simulations also show that to reduce contrast of undesirable local maxima and minima to $k \approx 0.1$, ratio $\frac{w}{a} = 1.1$ should be achieved.

However, this approach has its limitations. On one hand, for practical purposes is the beam size on the receiver's plane wider than receiving aperture to avoid signal to noise ratio reducing due to effects in turbulent atmosphere. On the other hand, there is limitation in the size of the lens, that must be smaller to reduce its aperture defect as well as its focus length is for manufacturing reason double of its diameter. In practice, the beam is slightly divergent, e.g. in the order of miliradians to satisfy both limitations mentioned above.

7   CONCLUSION

In the master's thesis scalar theory of diffraction was introduced as well as qualitative and quantitative analysis of diffraction effects in far-field and near-field with emphasis on region of Fresnel diffraction. Furthermore, Fresnel approximation of Rayleigh-Sommerfeld integral was introduced as the main approach to Fresnel diffraction effects modelling. Terms Fresnel number and Fresnel zone were described. In the end, derivation of diffraction integral was mathematically derived.

Following part deals with description of Gaussian beam as the most widely used approximation of real laser beams. Its main parameters beamwidth w and radius of curvature R were introduced and used to determine complex parameter of the beam $\dot{q}$. For better approximation of real laser beams, elliptically symmetrical Gaussian beam was described.

Main part of thesis describes simulation of diffraction effects. Two approaches are developed. First, based on integration of Bessel function brings limitations to only circularly symmetrical cases. Second, based on calculation of Fourier transform of the incident wave is taken as the main approach and it was embedded in GUI in MATLAB enviroment.

In the following part, both simulations were confronted with real experiment. There were limitations for the experiment discussed and layout of the experiment proposed and realised accordingly. Both simulations were confirmed and limits for their application were discussed. Additionaly, measurement error was estimated and its impact on measured results were discussed.

In the final part, deviations of measured intensity distribution from simulated are discussed. As the main source of error precision of collimation was identified. Furthermore, method how to estimate Fresnel number was proposed as it causes many troubles when real diffraction patterns are observed. Within this context, method of estimation of contrast was discussed. Additionaly, differences between geometrical and diffraction divergency and its estimation were introduced. In the end, consequences of Fresnel diffraction in practice were identified. Proposed method of reducing its effect requires use of non-planar wave.

Following effort will be focused on introducing divergent beam representation and study of multiple beam propagation and its use for beamshaping on the plane of receiver.

BIBLIOGRAPHY

[1] KOMRSKA, J. *Difrakce světla.* Text přednesený v rámci předmětu "Vlnová optika" studentům 4. ročníku oborů "Fyzikální inženýrství" a "Přesná mechanika a optika" v zimním semestru šk. r. 1999/2000, Brno:FSI VUT v Brně 2000.

[2] WILFERT, O. *Optoelektronika.* Elektronické skriptum. Brno: FEKT VUT v Brně, 2008.

[3] ALDA, J. *Laser and Gaussian Beam Propagation and Transformation. Encyclopedia of Optical Engineering.* New York: Marcel Dekker, Inc., 2003 - [cited 1.5.2010], p. 999 - 1013.

[4] ŠEBESTA, J., SMÉKAL, Z. *Signály a soustavy.* Elektronické skriptum. Brno: FEKT VUT v Brně, 2007.

[5] KOMRSKA, J. *Fourierovské metody v teorii difrakce a ve strukturní analýze.* Text přednášek pro 3. ročník magisterského studia "Fyzikálního inženýrství" a 4. ročník magisterského studia "Přesné mechaniky a optiky" v letním semestru šk. r. 1999/2000, Brno:FSI VUT v Brně 2000.

[6] SVĚTLÍK, J. Simple Methods for the Measurement of Laser Beam Parameters. *Applied Optics.* June 1974, vol. 13, no. 6, p. 1276 - 1278.

[7] WILFERT, O., KOLKA, Z. Statistical model of free-space optical data link. In: *Proc. of The International Symposium on Optical Science and Technology.* Conference 5550. Denver: SPIE. 2004, p.203-213.

[8] SALEH, B. E. A. *Základy fotoniky.* Praha: Matfyzpress, 1995. ISBN 80-85863-00-6

LIST OF SYMBOLS, PHYSICAL CONSTANTS AND ABBREVIATIONS

CCD Charge-coupled device

FFT Fast Fourier Transform

FT Fourier Transform

GUI Graphical user interface

He–Ne Helium-Neon

MATLAB Matrix Laboratory

PAT Pointing, Acquisition, Tracking

a Distance from light source P_0 to shielding object μ

b Distance from shielding object μ to plane of observation π

C Arbitrary constant

circ Circular function

D Diameter

Δ Difference

$\Delta\lambda$ Spectral width

δ Deviation

e Exponential function

exp Exponential function

$\mathcal{F}$ Fourier Transform

f Focal length

f_{mod} Modulation frequency

I Intensity

$I_{\max}$ Maximal intensity

$I_{\min}$ Minimal intensity

j Imaginary constant

J_ν Bessel function of the first kind of ν-th order

k Wave number

k Magnification constant of objective

k Contrast

$K(\vartheta)$ Slope factor

λ Wavelength

M Center of secondary waveform

μ Plane of shielding object

n Number of Fresnel zones

n_x Direction cosine

n_y Direction cosine

N_f Fresnel number

P Point of observation

P_0 Plane of light source

P_1 Point source

π Plane of observation

ϕ Angle from the x axis to the point of observation P

ϕ_0 Sum of spherical waves coming to point of observation

ϕ_M Angle from the x axis to the point of diffraction M

$\psi_0(M)$ Wave function of incident wave on the plane of diffraction aperture

$\psi(x, y)$ Distribution of wave function in determined plane

$\dot{q}$ Complex beam parameter

R Radius of curvature

r Radius

ρ	Distance from the origin to the point of observation P
ρ_0	Radius of diffraction aperture
ρ_M	Distance from the origin to the point of diffraction M
S	Plane of diffraction aperture
S_0	Part of the diffraction aperture plane
s_0	Direction from the origin 0 to S
s_M	Direction from the point M to S
σ_0	Spherical wave
θ	Beam divergency
ϑ	Angle between normal to a wavefront at the point M and the direction determined by the connection of the point M and the point of observation P
u	Spatial Frequency in x axis
v	Spatial Frequency in y axis
V_{pp}	Peak to peak voltage
w	Beamwidth of beam
w_0	Beamwidth on the plane of beam waist
w_x	Beamwidth of beam in x axis
w_y	Beamwidth of beam in y axis
x	x axis
x_M	x coordinate on the plane of diffraction
x_m	Quantity in real units
x_p	Quantity in display units
y	y axis
y_M	y coordinate on the plane of diffraction
Z	Source of light

Z_ν Bessel function of ν-th order

z z axis

z_0 Rayleigh distance